BRNO UNIVERSITY OF TECHNOLOGY
VYSOKÉ UČENÍ TECHNICKÉ V BRNĚ

FACULTY OF MECHANICAL ENGINEERING
INSTITUTE OF MATERIALS SCIENCE AND ENGINEERING

FAKULTA STROJNÍHO INŽENÝRSTVÍ
ÚSTAV MATERIÁLOVÝCH VĚD A INŽENÝRSTVÍ

OXIDATION BEHAVIOR ADJUSTMENT FOR TiAl INTERMETALLICS BY CONTROLED ATMOSPHERE SURFACE REMELTING

ÚPRAVA OXIDAČNÍCH VLASTNOSTÍ TIAL INTERMETALIK PŘETAVOVÁNÍM POVRCHU V ŘÍZENÉ ATMOSFÉŘE

MASTER'S THESIS
DIPLOMOVÁ PRÁCE

AUTHOR **BC. JANA PREHRADNÁ**
AUTOR PRÁCE

SUPERVISOR **DOC. ING. VÍT JAN, PH.D.**
VEDOUCÍ PRÁCE

BRNO 2014

Vysoké učení technické v Brně, Fakulta strojního inženýrství

Ústav materiálových věd a inženýrství
Akademický rok: 2013/2014

ZADÁNÍ DIPLOMOVÉ PRÁCE

student(ka): Bc. Jana Prehradná

který/která studuje v **magisterském navazujícím studijním programu**

obor: **Materiálové inženýrství (3911T011)**

Ředitel ústavu Vám v souladu se zákonem č.111/1998 o vysokých školách a se Studijním a zkušebním řádem VUT v Brně určuje následující téma diplomové práce:

Úprava oxidačních vlastností TiAl intermetalik přetavováním povrchu v řízené atmosféře

v anglickém jazyce:

Oxidation behavior adjustment for TiAl intermetallics by controled atmosphere surface remelting

Stručná charakteristika problematiky úkolu:

Intermetalické slitiny na bázi TiAl jako perspektivní konstrukční materiály pro vysokoteplotní aplikace jsou limitovány malou odolností vůči oxidaci při teplotách převyšujících 700°C. Při delších expozicích dochází navíc k porušování již vzniklých oxidických vrstev, což vede k prohloubení oxidace prvků tvořících intermetalickou slitinu a zkřehnutí základního materiálu.
Práce bude zaměřena na možnosti ovlivnění povrchu experimentální intermetalické slitiny s cílem tvorby stabilních oxidických vrstev.

Cíle diplomové práce:

Cílem úkolu je experimentálně ověřit možnosti ovlivnění oxidační odolnosti materiálů na bázi TiAl intermetalik přetavením jejich povrchu působením laserového nebo elektronového paprsku v kontrolované atmosféře, především s vysokým obsahem dusíku. Pro splnění úkolu je nutné provést teoretickou studii odborné literatury, připravit a provést experimenty přetavování a následné dlouhodobé vysokoteplotní expozice. Výsledky experimentů budou hodnoceny metodami strukturní a fázové analýzy a měřením lokálních mechanických charakteristik.

Seznam odborné literatury:

[1] Fiala, J., Kraus: I. Povrchy a rozhraní, ČVUT v Praze, Praha 2009.
[2] Wu X., Huang A., Hu D. Lorreto MH: Oxidation induced embrittlement of TiAl alloys, Intermetalics, 17, 2009, pp. 540-552.
[3] Froelich M., Ebach-Stahl A., Braun R., Leyens C: Oxidation protective coatings for TiAl – recent trends, Mat. Wiss. u. Werkstofftech., 2007, 38, No. 9, p. 667-673.

Vedoucí diplomové práce: doc. Ing. Vít Jan, Ph.D.

Termín odevzdání diplomové práce je stanoven časovým plánem akademického roku 2013/2014.

V Brně, dne 22.1.2014

L.S.

prof. Ing. Ivo Dlouhý, CSc. Ředitel ústavu	prof. RNDr. Miroslav Doupovec, CSc., dr. h. c. Děkan fakulty

ABSTRACT

This master's thesis deals with research of technological processing method called surface melting. The first part deals with the melting process and the basic parameters influencing the process of melting. In the second part, there is mentioned the comparison of two basic types of lasers namely Nd: YAG and CO_2, which was used for experiment in our case. The third part deals with the properties of TiAl intermetallic alloys, preferably α-phase γ-TiAl and Ti_3Al.

Finally it is made reference to the oxidation of TiAl alloys. The experimental part is devoted to melting the surface alloy Ti-46Al-0,7Cr-0,1Si-7Nb-0,2Ni in a controlled nitrogen atmosphere. It was necessary to do several measurements to find out the relevant parameters for the desired results. After the parameters were obtained, measurements of microhardness were performed. The last step of our experiment was to measure the increase of weight of samples due to oxidation process.

Keywords: melting process on the laser, intermetallics alloy TiAl

ABSTRAKT

Rešerše se zabývá teorií technologického způsobu zpracování materiálů, tzv. povrchového tavení. V první části rešerše je popsána samotná technologie a základní parametry ovlivňující proces tavení. Ve druhé části je uvedeno srování dvou základních typů laserů, a to Nd:YAG a CO2 laser. CO2 laser byl použit v případě našeho experimentu. Třetí část se zabývá vlastnostmi TiAl intermetalických slitin, především jejich fázemi α-TiAl a γ-Ti_3Al. Na závěr teoretické části je zmíněna oxidace TiAl intermetalických slitin.

Experimentální část je věnována přetavování povrchu slitiny Ti-46Al-0,7Cr-0,1Si-7Nb-0,2Ni, a to v ochranné atmosféře dusíku. Tato část obsahuje výsledky několika experimentů, na jejichž základě bylo nutné stanovit potřebné parametry pro požadovaný proces tavení. Posledním krokem experimentu byla snaha o zvýšení hmotnosti vzorků v důsledku následné oxidace.

Klíčová slova: proces tavení pomocí laseru, intermetalické slitiny TiAl

BIBLIOGRAPHIC CITATION

PREHRADNÁ, J. *Oxidation behaviour adjustment for TiAl intermetallics by controled atmosphere surface remelting*. Brno: Brno University of Technology. Faculty of Mechanical Engineering, 2014. 63 p. Supervisor of master's thesis: doc. Ing. Vít Jan, PhD.

COPYRIGHT NOTICE

I confirm that this master's thesis was written independently, based just on the literature listed at the end of this document and according to the direction of supervisors of my thesis.

Brno 30th May 2014 _____

Student's signature

ACKNOWLEDGEMENTS

First of all, I would like to express my sincere gratitude to my project supervisor Dr Ing. John C. Betts for facilitation this work on the University of Malta, sharing with me his knowledge and experiences and for his encouragement and patience throughout the work on this project. I would like to thank also doc. Ing. Vít Jan, Ph.D. from Brno University of Technology for his support with my foreign research fellowship throughout the project and for his continuous advices and helpful comments during whole time.

Special thanks also go to Mr. Clayton Damato from University of Malta who helped me with work on the laser a lot. Without his assistance and experiences I wouldn't be able to do this work. He was always available whenever help was required.

Last, but not least, I would like to thank my parents, who supported me during my whole study, not only financially but psychically as well. I would never finish this study without them.

Table of Contents

1 INTRODUCTION

Titanium alloys have been developed on a large scale as commercial alloys during 60 years, fulfilling the requirement for materials with high strength-to-weight ratios at elevated temperatures, initially used in the aerospace and defence industries. In these industries it is used over 80% of titanium alloys, mostly in the wrought form. Many other applications are restricted because of their low tribological and oxidation properties. Titanium alloys have high relative price, it is about five times that of steels and aluminium alloys. Titanium alloys have prominent corrosion resistance in sea water environments and in rainwater, because of the formation of protective oxide films. These films have been recognized and utilized by the chemical industry and also have led to applications in the medical profession in prostheses for implanting in the human body or in dentistry. Titanium has a high melting point – 1678°C, which indicates that the titanium alloys shows good creep resistance over a significant range of temperatures. [2]

Intermetallic alloys based on TiAl are considered as materials with the “progressive” structure. They are advanced materials for high temperature structural applications in the automotive industry, aerospace and energetic. Their disadvantage is the limited resistance to oxidation at the temperatures exceeding 700 °C. It should be noted that at these and higher temperatures is appeared a sharp decline in mechanical properties, even after a short exposure. In consequence of long-term oxidation there is the breach of protective oxide layer on the surface. [15] One of the most interesting phases of TiAl intermetallics is γ-TiAl phase. The attractiveness γ-TiAl lies in its low density, high purity (impurities can be achieved up to >99,5%), high strength (~650 MPa), increased stiffness, higher thermal conductivity and higher melting temperature (~1460 °C), good oxidation properties and still the improving resistance to creep at high temperatures.[15], [20]

Laser surface melting of light alloys requires the application of a laser beam in continuous (constant power with time) or pulsed wave or mode to melt a small area with a shallow depth on the material surface and afford it to re-solidify by cooling by the cooler bulk of the material once the as soon as ever beam has moved on. An inert atmosphere is required if any form of reaction (usually reaction with atmospheric nitrogen or oxygen) is to be bewared, and this is reached by using a jet of shielding gas or by carrying out the process in a controlled environment. The melting process by laser produces three profitable results in the re-solidified material. The first useful result is grain refinement. It can increase the resistance to wear and surface hardness. The second result is a more homogeneous redistribution of alloying elements within the alloy. Homogenization is usually beneficial to corrosion resistance as a consequence of the elimination of isolated phases of alloying. The last important effect is the creation of intermetallic phases resulting from reactions of alloying metals in the laser-created molten pool. One of the characteristics of the technique as is the laser surface melting is the very fast solidification, which can produce hardening through the introduction of crystalline defects, such as dislocations and vacancies. Often residual stresses, which result in a distortion of the work-piece, are occurred, but this can be surpassed by the application of a low-powered surface heating procedure following the laser melting process. [10]

2 LITERATURE REVIEW

2.1 Laser melting surface

The process whereby the alloy surface is laser melted and then re-solidified without any attempt to modify the surface layer chemical composition is normally referred to as laser melting. [10]

Surface melting processes are currently not as widespread as transformation hardening since they are processes that rely on transformation to the liquid state, with the attendant change in surface absorptivity and the difficulty in maintaining a constant absorbed energy for consistent and reproducible processing. [1] But it depends; surface transformation hardening is generally applied only to steels, whilst melting has a wider range of application.

The main benefits of surface melting is originates from the ability to produce fine remelted microstructures with good wear, oxidation properties and corrosion. A variant process based on the principles of melting procedural variation is associated with the techniques of adding alloy materials. [1]

Processes based on laser surface melting provide unique means of precisely controlling the formation of microstructures. The surface chemistry can be adapted to specific applications. Once process automation becomes more widespread, the processes will have much to offer for industrial application particularly in small-scale applications for which there are few conventional methods of accurate localized melting that also have the potential for contemporaneous alloying. [1]

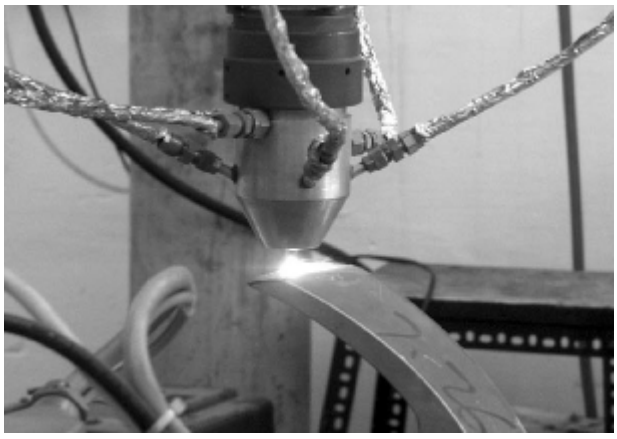

Fig. 1.CNC laser beam cladding over a complex surface [10]

2.1.1 Processes with material during melting

In surface melting the near-surface area first rapidly reaches the melting point and a liquid/solid interface starts to move through the alloy. Diffusion of elements begins in the liquid phase. The presence of the laser in the area of effect is nearly terminated while the surface has remained below the vaporization temperature. At this stage the

maximum melt depth has been attained, interdiffusion continues, and the re-solidified interface velocity is momentarily zero and then rapidly increases. The interface moves back to the surface from the area of maximum melt depth. Interdiffusion continues in the liquid, but the re-solidified metal behind the liquid/solid interface gets cold so fast that solid state diffusion may be irrelevant. By the last stage, re-solidification is finished and a surface alloy has been created. The re-solidified alloy has on the surface a film of titanium oxide. This film confers good wear resistance. [10]

2.1.2 The process variables

Successful application of laser melting requires an understanding of the principles of the process and appreciation of the effect of practical process variables on the properties of the processed material. We can consider the process variables in three groups: material properties, beam characteristic and processing parameters. [1]

- **Material properties with a focus on Titanium**

Titanium can be remelted with added elements that possess a number of critical properties. They should form a hard phase rich in titanium to minimize the alloy concentration. The hard phase should form through primary solidification since solid state diffusion is limited with the high cooling rates involved. By remelting the added elements should have sufficient solubility in the α or β phase to allow solid solution hardening and to retain ductility. Alloying with carbon makes dendrites of TiC form. By melting in a nitrogen atmosphere, surface alloys of TiN dendrites in a α-Ti matrix can be produced with a golden color and hardness up to 2000HV. The strengthening intermetallic Ti_3Al is formed by adding aluminum to a molten titanium surface. [1]

- **Beam characteristic**

Wavelength

For many years, only CO_2 laser beams were able to deliver the combination of power density and interaction time necessary for remelting. Multikilowatt Nd:YAG and diode lasers, with shorter wavelengths, now provide significant advantages; as the beam wavelength decreases, the absorptivity of a metal surface increases and so an absorptive coating might not be necessary. This simplifies the operation substantially – the cost of applying and removing absorptive coatings is the factor the makes CO_2 laser remelting uneconomical in comparison with other methods of surface adjustment. [1]

Power

The power level used normally lies in the range 1 - 3kW. A high power level enables high traverse rates to be used, with correspondingly high coverage rates. However, the practical window of traverse rate is then reduced because the risk of both overheating, leading to surface melting, or insufficient peak temperature with no melting, increases. The robustness of the process is thus reduced. For these reasons an incident power of about 1 kW is normally recommended. Materials of high harden

ability may be processed with a lower power density and a higher interaction time, in order to achieve a homogeneous case with significant depth. Conversely, materials with low hardenability are processed with higher power density and lower interaction times. [1]

- **Processing parameters**

Process gases

Process gas serves two functions in remelting. It shields the interaction zone, thus preventing oxidation, which can increase absorptivity in an undesirable, uncontrollable manner, and which may result in overheating or melting. The process gas also protects the optics from smoke and any other contaminants produced during processing. Nitrogen is common choice since its relatively high density blanket the interaction zone effectively. The same applies to Argon. Gas flow rates of around 20 l/min are normally used, depending on the area to be covered, delivered either coaxial with the beam or from an external spout. [1]

Most applications of melting are carried out using a fixed set of processing parameters. However, there may be occasions when changes need to be made to processing variables during the treatment. Such changes may me intentional – the section size of the component may change significantly – or unintentional – properties of the surface coating may change as a result of processing. System for controlling the temperature at the surface of a component has been constructed to adaptively control laser melting. The surface temperature can be measured using a pyrometer, and used to calculate the transformed depth by means of a mathematical model. [1]

2.1.3 Laser nitriding

This technique was initiated by the work of Katayama at al. and since that time have been there a number of such investigations.
Laser nitriding is in general gained by a reaction between nitrogen producing nitrides and a laser molten top layer. These nitrides after solidification become a hard composite layer with low coefficient of friction.

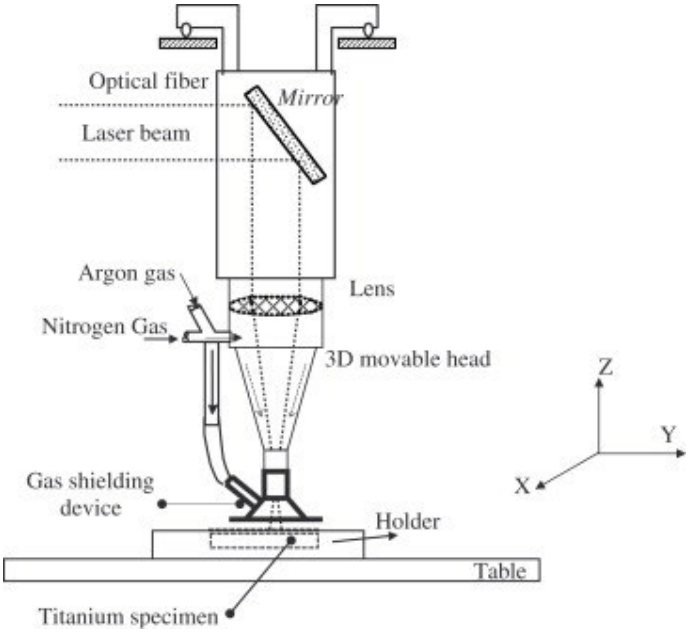

Fig. 2.Schematic diagram of the laser nitriding experimental set-up

Fig. 2 shows schematically us the experimental set-up of a laser gas nitriding process. The laser beam is reflected by mirror in the direction of specimen and it is focused by the lens to a point about 100 mm under the nozzle and 10 – 15 mm above the surface of a specimen. The flow measure of nitrogen gas is controlled using two calibrated flow metres: one for argon and second for nitrogen. The sample is fixed on the table by putting it into the holder to prevent movement during the process. [19]

2.2 Laser

Lasers are one of many tooling that have been used to modify the surface of alloys. They involve light amplification by stimulated emission of radiation, which gives advancement to the acronym laser. [2] The different types of laser can be classified according to the following criteria:

- The different types of laser that are used - their active medium (gas, liquid or solid), power, wavelength, mode of operation (continuous or pulsed) and energy;
- The variety of materials treated - metals and alloys, glasses and ceramics, polymers and composites;
- The mode of beam-material interaction - thermal (induced by heat transfer – melting, heating and vaporization) and athermal (induced by changes on the atomic scale - making and breaking chemical bonds);
- The myriad applications that have been developed from a limited palette of processing mechanisms [1]

Gas media include atoms, molecules, ions and excimers. The basic liquid media present organic dyes. Solid media comprise insulating crystals and semiconductors. [1]

2.2.1 Carbon Dioxide (CO2) laser

John C. Ion imputes the popularity of carbon dioxide laser to its efficient use of gases, which reduces running costs, that the pulsed or continuous wave emission is produced in a high quality beam at super kilowatt power levels, and that far-infrared light is transmitted readily in air, being absorbed by a wide range of engineering materials. However, he expects there to be a growth in the use of multi kilowatt diode-pumped solid state lasers (DPSS), which offer compactness, high power efficiency and high beam quality. [2]

The CO_2 laser (invented by Kumar Patel of Bell Labs in 1964) was one of the earliest gas lasers to be developed and is still one of the most useful. [9] The design, which is relatively simple and robust, is scaled easily to high power levels. [1] The carbon dioxide laser is the highest-power continuous wave laser that is momentarily at disposal. [9]

In a CO_2 laser generally in a mixture with: Nitrogen N_2 (around 10 – 20%), Hydrogen H and/or Xenon Xe (a few percent; usually used only in a sealed tube) and Helium He_2 (the remainder of the gas mixture), generates the beam. Helium is the major part of this mixture due to its high thermal conductivity and the role of Helium is in cooling. The gas pressure, at which most of CO_2 lasers operate, is approximately one-tenth of atmospheric pressure. Electrodes or RF coupling are used to deliver electrical energy to the gas mixture. The specific admeasurements change into according to the concrete laser. [11]

CO_2 lasers can be continuous-wave or pulsed, while both capabilities, in many cases, are existing in a single unit. The operating power in a continuous-wave operating laser is equal to its average power. In a pulsing laser, the average power is enhanced as a top power and is regulated by an on/off duty cycle. [11]
A continuous-wave CO_2 laser can also be combined with a beam-steered delivery system. The CO_2 lasers emit a narrow bandwidth of light in the far infrared wavelength at 10.6 μm. This wavelength is most preferable to for ceramics, plastics and organic materials, such as paper and other wood products. [11]

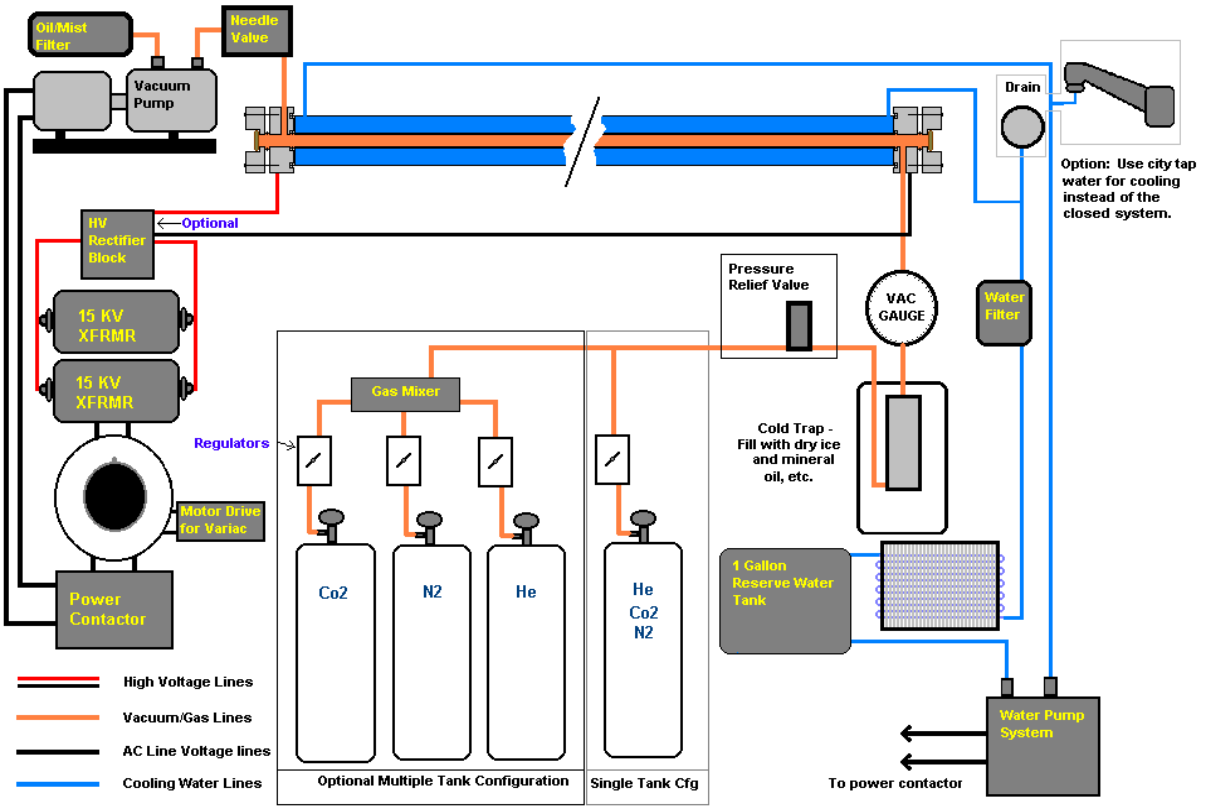

Fig. 3. CO_2 Laser Basic System Diagrams [13]

2.2.2 Nd:YAG vs. Carbon Dioxide (CO2) lasers

Nd:YAG and Carbon Dioxide (CO_2) lasers emit radiation at different wavelengths. Fundamentally, the 1.064 micron wavelength of the Nd:YAG is an order of magnitude shorter than the 10.6 micron radiation from a CO_2 laser. In materials processing, the shorter wavelength of the Nd:YAG couples better to metal while the longer CO_2 wavelength is more suitable for cutting ceramics, plastics and organic materials. [3] However, the inherently higher power and ability to focus CO_2 lasers make that the most commonly used laser for thick metal cutting, deep penetration welding and high-speed production. [11]

CO_2 lasers provide higher (more efficient) conversion of electrical power into laser power than Nd:YAG lasers. [11]

CO_2 lasers are typically less expensive in equipment cost, and generally have lower operating costs, while Nd:YAG lasers in general have less extensive, simpler maintenance requirements. [11]
Due to the requirement for high-frequency, only the pulsed Nd:YAG laser is available to developed shock processing. By a CO_2 laser is not possible to produced so short-pulse laser impulses. [10]

Many areas of cross-over in the applications of CO_2 and Nd:YAG lasers are there and some exceptions to the general statements above. The benefits for either technology should always be considered on a case-by-case basis. [11]

2.3 Titanium

The element titanium was discovered in 1770, but its applications came later. People started to perceive useful properties of this element after 1950. Since then it is titanium widely used in industrial practice and design applications. It found a lot of the uses also in military and gas turbine engines. Titanium is used today for its corrosion resistance, unique density, and relative strength advantages competing with steels, aluminium and also super alloys. [22] Titanium's density is 4,507 kg/m^3 and it means it is 60% lighter compared to steel. [23] The ratio between density and strength is 240MPa, this value is relatively good. [24] This element has low thermal conductivities and very high electrical resistance. [25] The big advantage of titanium is certainly also its biocompatibility. [24]

Titanium is in general very expensive due to the high cost of production. The biggest requirement of the production of titanium is its production in vacuum or inert atmosphere because of its high reactivity with oxygen. [24] This reactivity is actually useful because of thin layer of oxide TiO_2 which are created on surface due to oxidation. The oxid TiO_2 stays stable of up to 600 °C, so applications of using titanium are limited by this temperature. It exists a few methods which propose improving the oxidation resistance of TiAl alloys. Most of studies dealing with this problematic are concerned with the influence of ternary and quaternary additions. [26]

2.3.1 Crystal structure of titanium and titanium alloys

The melting point of pure titanium is 1660°C. Nevertheless most of commercial alloys are used under 538 °C. [22] Pure titanium has polymorph structure. In the case when the temperature is raised above 882,5 °C, the structure of titanium is changed from HCP α to BCC β. This conversion influences tensile strength, elastic modulus and also oxidation resistance. [27] For different properties it can be used different environments.

- The titanium with HCP α

The titanium alloys with HCP α is mostly used for aircraft parts and for cryogenic equipment. The main advantage is its resistant to brittle fractures. It has low density and high strength of up to 1000 MPa. It shows good mechanical properties at temperature beyond 300 °C. These alloys are not suitable for heat treatment. [28]

- The titanium alloys with BCC β

These alloys have a good corrosion resistance, good hardenability and can be formed at room temperature. Tensile strength after heat treatment can reach up to 1600 MPa. These group of titanium alloys are more heavier than other titanium alloys due to higher density, which is ranging from 4800 to 5050km/m^3.[28]

2.4 Intermetallic titanium alloy - aluminides

Intermetallic titanium aluminides offer an attractive combination of low density and good oxidation and ignition resistance with unique mechanical properties. Accordingly, they are one of the few classes of emerging materials that have the potential to be used in demanding high-temperature structural applications whenever specific strength and stiffness are of main concern. Advanced TiAl alloys have very complex microstructures with very important features at the nanometer scale. There is an intimate correlation between the alloy chemistry, constitution, microstructure and mechanical properties, which has to be considered for the purpose of to meet the desired properties. [4]

Intermetallic titanium alloys are based on a so called intermetallic phase. From technical interest are TiAl, Ti_3Al, Al_3Ti and Ti_2AlNb. The properties of intermetallics are in some way in between metals and ceramics. They show excellent high temperature properties but less ductility than conventional metals. [5] Intermetallic titanium alloys are characterized by high resistance against the thermal and stress exposure. [6] They have the low density, good strength limit in the higher temperatures and very good corrosion resistance. Particularly the favorable ratio strength/density makes it very attractive in terms of the applications in air and missile technology and the automotive industry. [7] Intermetallics TiAl based - and Ti_3Al are currently very intensively examined.

The last few years have been developed alloys with higher content (3-10%) of Nb alloying element in order to improve the oxidation resistance and the tensile strength, such as the alloy: Ti-46Al-7Nb-0,7Cr-0,1Si-0,2Ni (at.%). [8]

2.4.1 Intermetallic phases α-TiAl and γ-Ti3Al

Phase α-TiAl characterizes excellent properties like high temperature strength, creep resistance and oxidation, low density and high fatigue resistance. However α-TiAl shows a low ductility. This must be considered during component designing and it is the major hurdle for a widespread use for many applications.

Alloy α-TiAl is used for some high temperature near-net-shape components. It is from interest for applications like jet engine blades, compressor wheels for turbo chargers, automotive valves and other high temperature components. For high temperature application requiring low weight it is a good alternative to super-alloys up to 850 °C. [5]

Like α-TiAl, alloys based on the intermetallic phase γ-Ti_3Al featuring also creep resistance and high oxidation. The strength levels of tensile and fatigue are much higher than for α-TiAl. The density is higher than for α-TiAl, around 4 g/cm³, but somewhat lower compared to the Ti_2AlNb phase. The maximum temperature for long term service is around 750 °C. Dependent on the microstructure γ-Ti_3Al alloys could show high ductility values up to 20%. [5]

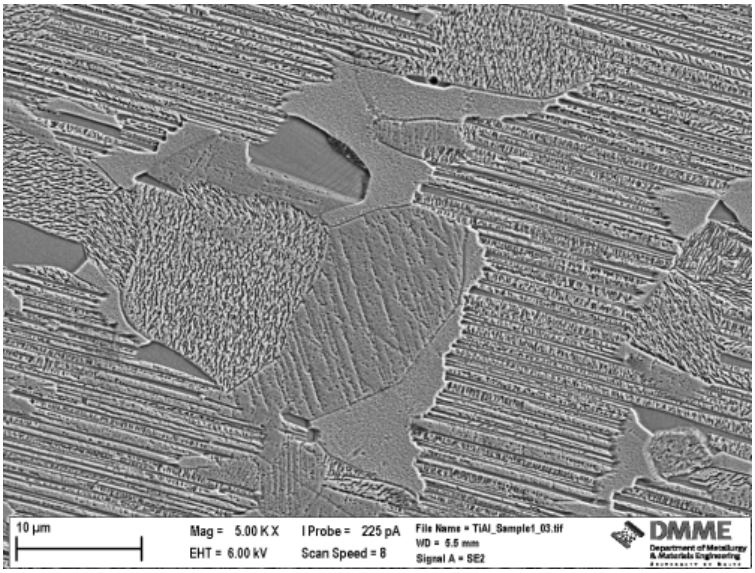

Fig. 4.Intermetallic phases α-TiAl and γ-Ti_3A

Table 3.1 summarises a comparison of the mechanical properties α-TiAl and γ-Ti_3Al. [6]

Tab. 3.1 *The compare of mechanical properties phases α-TiAl and* ***γ-****Ti_3Al*

Properties	**Phase α-TiAl**	**Phase γ-Ti_3Al**
Density [g/cm^3]	4,1 – 4,7	3,4 – 4
E - Young's modulus of elasticity [GPa]	120 – 145	160 – 175
Ductility [%]	2 – 5	1 – 3
Limit of elasticity [MPa]	700 – 900	400 – 650
Temperature conductivity [W·m^{-1}·K^{-1}]	7	22
Max temperature of stability [°C]	1180	1440
Creep limit [°C]	750	900
Limit of oxidation [°C]	650	900

2.4.2 Ti-46Al-7Nb-0,7Cr-0,1Si-0,2Ni

This alloy is one ot the most ordinarily used alloys from intermetallic alloy based on Ti-Al, it has duplex microstructure. This microstructure is compozite of γ-TiAl and α_2-Ti_3Al phases, as is shown on Fig 5.

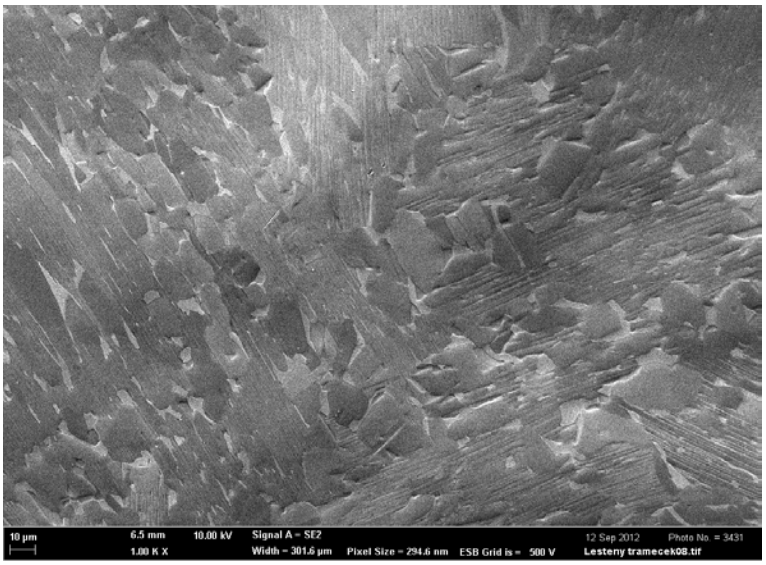

Fig. 5.Microstructure of Ti-46Al-7Nb-0.7Cr-0.1Si-0.2Ni

On mapping analysis of the concentrations of elements it is seen higher content not only of Ti, but also Al, Cr, Ni and Nb - Fig.6. The addition of Nb is there because of improving resistance to oxidation. This alloy is very predisposed to surface inequality. This alloy has 50 a/w ration of Al and Ti, but because of its thermodynamic character it is preferentially formed porous oxide - TiO_2 instead of Al_2O_3 oxide, which could be used for protection. [29]

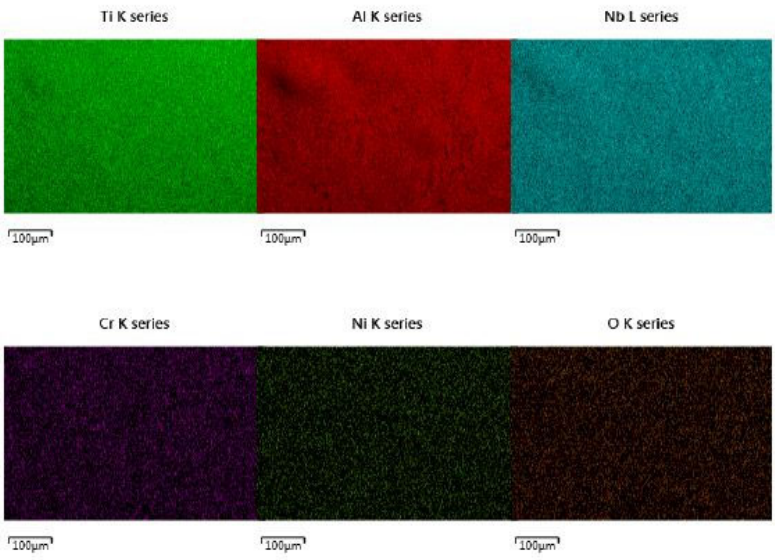

Fig. 6. Mapping analyses of Ti-46Al-7Nb-0.7Cr-0.1Si-0.2Ni

2.4.3 Third generation alloys with high niobium-contents

Over the last years, the research is focussed on alloying Ti_3Al and TiAl with high content of Nb, which supports to substantial improvement of the oxidation resistance. At the present time, the chemical composition of Ti-Al intermetallic-based alloys with high Nb-contents (third generation alloys) is s forming by the following rule [12]:

$$Ti - Al_{42-46} - Nb_{4-10} - X_{0-3} - Y_{0-1} - Z_{0,1} - RE_{00,5}-$$

, where X – contents of Mn, Cr and Ta;
Y – contents of W, Hf and Zr;
Z – contents of Si, C and B;
RE – rare earth elements.

It was proved that niobium alloying improved oxidation resistance, because: Nb increases the thermodynamic activity of Al relative to that of Ti, which favours the formation of a stable alumina scale; Nb ions replace Ti ions, i.e. TiO_2 is doped by Nb, that is leading to a decrease in oxygen vacancies and in consequence to slowing diffusion of oxygen; Nb lowers the solubility of oxygen in the alloy, thus restraining the internal oxidation of the alloy and promotes the formation of TiN on the interface, which inhibits the diffusion of oxygen and titanium ions. [12]

2.5 Oxidation

Oxidation is a reaction in which the atoms due the addition of oxygen in an element lose electrons and the valence of the element is correspondingly increased.

2.5.1 Resistance to oxidation TiAl intermetallics

In general, temperatures for operating conditions for TiAl-based alloys are between 700 – 800 °C. However, it is shown that after a short time exposure at 700 °C mechanical properties have dramatic losses. Removing material from the surface layer leads to restore the original values and mechanical properties. [14] It is evident that this behavior is associated with the characteristics of the surface and can be caused by a reaction between the metal surface and the atoms of atmospheric oxygen. [15]

Oxidation of TiAl intermetallics depends on the ratio of Al and Ti in the alloy. With increasing aluminum content is created four typical compounds: TiAl, Ti_3Al, Al_3Ti and $TiAl_2$. Unfortunately intermetallic phase with this composition doesn't form a stable continuous protective oxide layer on the basis of Al, which should protect the material against the oxidation. [17]

After that TiAl alloy is exposed to the atmosphere at high temperatures, titanium and aluminum oxides begin be formed. The stability of both types of oxides is very similar. The forming of oxides Al_2O_3 has a lower Gibbs energy than the forming of oxides TiO_2 and should therefore be considered as thermodynamically stable and should be more easily created. [16] Oxides on surface are formed more TiO_2 than

inhomogeneous Al_2O_3. When the material is exposed to the air, titanium starts form nitrides, which could be considered as a surface protection, but these nitrides mostly destroy the continuous aluminum layer. [17]

To the form a continuous protective layer of good quality must be guaranteed by the following criteria [15]:

- Emerging oxide should be thermodynamically stable, in order for prevent the formation of other undesirable phases in the near area.

- Growth of layer should be controlled by diffusion and should be guided by the rules parabolic growth.

- Layer should be easy to create on complicated surfaces and spalling should regenerate.

On the based of the experimental results the [12] published that confirm that the increase of the surface roughness (specified by Ra value), can improve the wear resistance against oxidation for the Ti–46Al–7Nb–0.7Cr–0.1Si–0.2Ni alloy tested. This experiment has been investigated in air at 900 °C, 925°C and 975 °C under cyclic exposure conditions.

2.5.2 Improve the oxidation resistance with alloying of elements

To improve the oxidation resistance of materials based on TiAl alloys contributes alloying elements. The effects of the various elements are shown in the periodic table belong to Fig.7. In general, the most beneficial alloying addition is niobium. In addition, to improving the oxidation resistance in Ti–Al–Nb alloys, niobium can offset the negative effects of other additions, such as small amounts of manganese or chromium. Niobium is often added also to improve the deformation characteristics of the material. It also states that niobium has a significant influence to support the creation of Al_2O_3 by improving the diffusion of aluminum in intermetallics. The other elements that appear to be most beneficial are tungsten, chlorine, silicon, silver and larger amounts of chromium. Concentration of chromium to the 4 Wt% increases the activity of aluminum and also forms the Laves phase, which acts as a diffusion barrier for oxygen and reduce the activity of titanium. Silicon provides limited protection by forming silicates of titanium or of titanium-aluminum, but these are gradually changing the SiO_2 particles and don't protect the material anymore. [17,30]

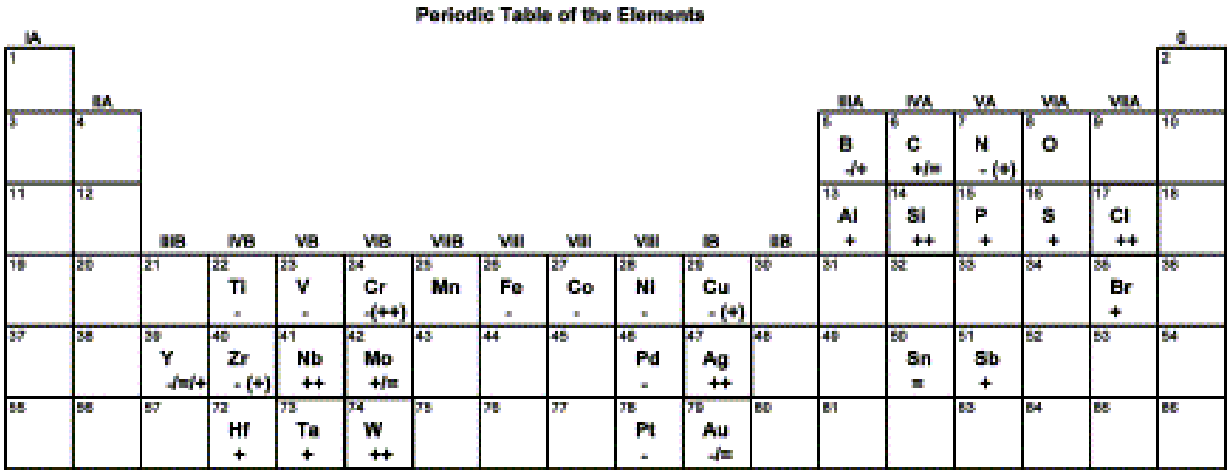

Fig. 7.The effect of alloying additions on the oxidation behavior of gamma titanium aluminide alloys. (+) beneficial, (-) detrimental, (=) neutral.

Nevertheless, the oxidation behavior of titanium aluminides is quite complex and various factors, such as interaction among alloying elements, microstructure, porosity, scale cracking, impurity level, surface finish and pretreatments, can significantly affect the oxidation behavior and complicate evaluation the environmental resistance of gamma titanium aluminide alloys.[30]

2.5.3 The improvement of oxidation resistance by coating

Until now, the studies and experiments conducted clearly show that TiAl alloys can be applied in aircraft or automotive engines because of their good mechanical properties in a wide range of temperatures. One of the limitations in introducing these materials on a mass scale is their very low oxidation resistance at temperatures above 800 °C. [31] It is an idea to protect the material by coating, which could help with oxidation resistance in higher temperatures.

In general, good preconditions for coating are very low permeability of oxygen, good adhesion, chemical and mechanical compatibility, excellent heat stability, thermal expansion and thermal conductivity of the substrate. It should be considered that the result of the coating is dependent on the used technologies. [15]

Gas phase aluminizing of TiAl intermetallics

The gas phase aluminizing technology enables producing a relatively thin coating of 10 μm and it is characterized by the multi-layer structure. In the case of the coating based on Ti46Al7Nb alloys, the composition of the phases is as follows: $TiAl_3$/$TiAl_2$/TiAl. [31]

In the outward of the coatings has been observed diffusion of the alloy elements to the surface zone. The niobium content is increased significantly in the inner zone of the coating, exceeding the content of that element in the matrix alloy. Despite its relative thin thickness, the aluminide coating obtained by out of pack method can constitute a perfect barrier, which is preventing the progress of the oxidation process

and which is free from any pores or fractures. The application of this technology provides the means for achieving the main purpose: the increase of aluminium content in the outer zone, which enables the formation of Al_2O_3 oxide, together with strengthening the oxidation resistance of the alloys. The gas phase aluminizing technology is possible to apply in aerospace industry, for example for the improvement of the oxidation resistance of turbine blades. [31]

PVD, EB-PVD, magnetron deposition methods

Physical Vapor Deposition is the method used to describe the group of coating processes. The most usual of these PVD coating processed are evaporation (typically by using electron beam sources or cathodic arc), and sputtering (by using magnetic enhanced sources or "magnetrons", cylindrical or hollow cathode sources). All of these processes must be performed in vacuum at working pressure (usually 10-2 to 10-4 mbar) and in general involve bombardment of the substrate to be coated with energetic positively charged ions during the coating process to support high density. Moreover, reactive gases such as oxygen, acetylene or nitrogen can be introduced into the vacuum chamber during metal deposition to create various compound coating compositions. The result is a very strong bond between the tooling substrate and the coating and tailored physical, structural and tribological properties of the film. [32]

In this case, these methods were used for creating MCrAlY coating and its modifications. Especially coating, which contains nitrogen, is an interesting possibility to protect material against oxidation during thermal cycling at temperatures above 750°C. The coatings TiAlN, CrAlYN, TiAlN + 8% YN and CrAlNY + 2 % YN provide oxidation resistance during thermal cycles in the interval from 750°C to 900°C. Instead of yttrium, it was also used silver, silicon and hafnium. Silver guarantees the formation of Z-phase in the initial stage of the thermal exposure. Silicon and hafnium change the coating TiAlCr at the cubic Laves phase (B2), which stabilizes the protective layer of Al_2O_3. It was also used EB- PVD process to create oxide diffusion barriers on the basis of Al + Y. The best resistance to isothermal oxidation was determined for layers in the ratio Al:Y as 1:2. In this case it was ultimately formed only protective Al_2O_3 layer on the surface of intermetallics. The oxide layer can be destroyed by the oxidation temperature shocks. The layer starts to crack and peel off. [15]

CVD, IBED

Chemical vapor deposition is a chemical process used to produce high-purity and high-performance solid materials. The process is used to produce thin films. In typical CVD, the substrate is exposed to one or more volatile precursors, which react or decompose on the substrate surface to produce the desired deposit. It can happen very often, volatile by-products are also produced, but they are removed by gas flow through the reaction chamber. [33]

In addition, the CVD methods can produce single layer, multilayer, composite, nanostructured and functionally graded coating materials with well controlled

dimension and unique structures at low deposition temperatures and in a short time [34]

The steaming by using chemical processes CVD, Ion-Beam enhanced deposition, coating by using a plasma jet deposition, sol-gel derivatives, dipping/coating process and some other techniques are also used for making glass-ceramic amorphous coatings. The ceramic coatings (Al_2O_3, Si_3N_4) have a favorable effect for the oxidation resistance of γ-TiAl alloys at 1000 ° C. The formation of thin ceramic films leads to a substantial decrease of the oxidation. [15]

3 OBJECTIVES

The aims of theoretical part of the thesis was to perform a literature research:

- Technological processing method as is surface melting
- The introduction to the theme of two basic types of lasers as are Nd:YAG and CO_2
- Discussion on TiAl intermetallic alloys
- Oxidation and resistance to oxidation TiAl intermetallics

The aims of practical part of this thesis were:

- To obtain the right parameters for the flawless surface melting by the laser in controlled atmosphere for the intermetallics alloy Ti-46Al-7Nb-0,7Cr-0,1Si-0,2Ni
- To determine the changes in the microstructure of the sample after melting
- To identify the changes in the microstructure of the material due to the subsequent oxidation with temperature 900 °C

4 EXPERIMENTAL PROCEDURES

4.1 Used material

The material used was titanium alloy Ti-46Al-0,7Cr-0,1Si-7Nb-0,2Ni. This material had 2 phases: near γ-TiAl and α_2-Ti_3Al. The exact composition of alloy is shown in Table 4.1.

The material was supplied by the company Flowers Corporation, Dayton as cast ingots. The diameter of the ingot was 70 cm. This ingot was cut on the small sample. The samples have form of small beams approx 3x4 mm cross and 50 mm length. These samples were used for our experiments – melting on the CO_2 laser in nitrogen atmosphere.

Tab. 4.1 *The composition of used material*

Elements	Ti	Al	Nb	Cr	Ni	Si	O	C	N	H
Wt.%	53,13	29,8	15,9	0,7	0,3	0,07	0,08	0,01	0,01	0
At.%	45,97	45,8	7,1	0,56	0,21	0,1	0,19	0,03	0,03	0,01

4.2 Melting

The laser, which was used in this investigation, was a CO2 laser operating in both continuous and pulse mode. The specifications of the laser can be used general as follows:

Name: Triagon 9000 laser
Manufacturer: Rofin-Sinar
Type: Class 4 CO_2 Fast Axial Flow
Max Power Output: 9 kW
Focal Length: 127 mm
Wavelength of radiation: 10,6 μm
Mode aperture Power Range :ON: 0.25 – 5 kW
OFF: 3.5 – 9 kW

The laser system was interfaced with a 4-axis CNC system.

The melting runs were carried out and any observations were noted. After every laser run, a new set of parameters was established to try and improve the result and melting obtained in the previous runs. Based on the results the following characteristics were changed in subsequent tests; the beam diameter on the sample surface, speed of movement on surface of the sample, flow of shielding gas and power of beam.

Laser runs were applied to two opposite sides of each sample.

Tables 4.2 – 4.5 show us the process parameters selected for all laser runs.

Tab. 4.2 *CW parameters used for samples*

Specimen	Diameter [mm]	Speed [mm/min]	Gas flow [l/min]	Power [kW]
1.1.	1	1000	20	1
1.2.	1	1000	40	1
2.1.	1	1000	30	1
2.2.	1	1500	40	1
3.1.	1	1500	40	1
3.2.	1	1500	40	1
4.1.	1	2000	40	1
4.2.	1	2000	40	1
5.1.	1,5	1000	40	1
5.2.	1,5	1000	40	1
6.1.	1,5	1500	40	1
6.2.	1,5	1500	40	1
7.1.	1,5	2000	40	1
7.2.	1,5	2000	40	1
8.1.	1	1000	40	1

Tab. 4.3 *Parameters used for samples for method pulsing*

Specimen	Diameter [mm]	Speed [mm/min]	Gas flow [l/min]	Power [kW]	Pulsing [puls/ms]
8.2.	1	1000	40	1	50
9.1.	1	1000	40	1	25
9.2.	1	1000	40	1	25

Tab. 4.4 *Parameters used for samples*

Specimen	Diameter [mm]	Speed [mm/min]	Gas flow [l/min]	Power [kW]
10.1.	2	1000	40	1
10.2.	2	1000	40	1
11.1.	2	1500	40	1
11.2.	2	1500	40	1
12.1.	2	2000	40	1
12.2.	2	2000	40	1

Tab. 4.5 *Parameters used for samples for method pulsing*

Specimen	Diameter [mm]	Speed [mm/min]	Gas flow [l/min]	Power [kW]	Pulsing [puls/ms]
13.1.	2	1000	40	1	50
13.2.	2	1000	40	1	25
14.1.	2	1000	40	1	50
14.2.	2	1000	40	1	25

4.3 Sample preparation

4.3.1 Mounting and grinding

Each of the samples was cut to across in two locations and then mounted in bakelite using a mounting press. Wet grinding of these samples was carried. Out to produce a uniform flat surface. Wet grinding was carried out using a graded sequence of abrasive papers (silicon carbide). The process was started with rough abrasive and progressed with softer ones, in the following sequence: 220, 400, 800 and 1200.

4.3.2 Polishing

Polishing steps were then required to produce a flat, reasonably scratch-free surface finish, using a machine very similar the ones used for grinding. Diamond abrasives, down to 1 μm particle size, were used for fine polishing whilst applying isopropyl alcohol (IPA) as a lubricant on a polishing cloth.

4.3.3 Etching

The samples were properly cleaned prior to etching so as to obtain a uniform etch effect on each of surface area. Etching was carried out so as to obtain a sharply defined contrast in the microstructure of the melting on our samples. Best results were obtained when etching using Kroll's reagent which consists of 6 ml nitric acid (HNO_3), 2 ml hydrofluoric acid (HF) and 92 ml distilled water.

4.4 Characterization

The samples were then examined and photographed under a Nikon optical microscope.
It was using a DFC 290 Leica camera affixed to it. In the second case was used for optical metallography the ZEISS Axio Observer Z1m and measurements was done using the Carl Zeiss Axio Vision software.
Chemical analysis was carried out by a LEO 1430 Scanning Electron Microscope and Carl Zeiss ULTRA plus Scanning Electron Microscope and Oxford Instruments X-MAX Energy Dispersive Spectroscopy (EDS) on selected sample.

4.5 Microhardness

Hardness profiles were taken using a Mitutoyo MVK – H2 micro-indentation hardness tester.
In this case the measurement of microhardness was achieved by sinking a Vickers diamond indenter (Fig. 8(a)) to the surface measured body by force 200g for a period 10s. Microhardness was measured on three positions (Fig. 8(b)) – basic material,

cross-over between basic material and melted zone, zone after melting. Basic material is measured always once on each samples. Other parts are measured twice on every part of sample.

a)

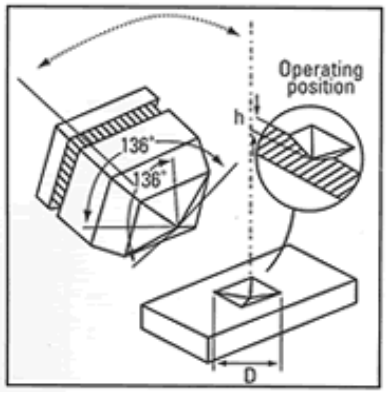

b)

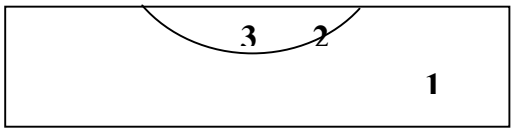

Fig. 8. Diamond body of Vickers form (a) [18] and positions of measurement (b)

4.6 Oxidation

A standard chamber furnace with heating elements and air atmosphere was used for oxidation heat treatment. The oxidation process was made at 900 °C for 100 hours. The furnace was switched off after 100 hours and samples were left to cool down slowly on their own.

4.7 Three point bend test

The three point bend test was taken on MASHINE. The distance between support points was 16 mm. The speed of the test was 1 mm per minutes. The three point bend test was implemented and evaluated according to standard.

4.8 Reflectivity of used material

Reflectivity of used material was measured on the spectrometer Varian Carry. The wavelength 500-2500 nm was used for determination useful results.

5 RESULT AND DISCUSSION

5.1 Chemical analysis

First and foremost, the mapping chemical analysis of the basic material (Ti-46Al-7Nb) was analysed, showing with the following microstructure. In the picture we can see two phases; near γ-TiAl and α_2-(Ti_3Al); the phase "near γ-TiAl" means that it is close to the gamma, but not exactly 50 percent. However, titanium is seen to comprise more than 50% of the alloy. Phase α_2-Ti_3Al is fragile and the structure is cracked, this is clearly represented in Fig. 9.

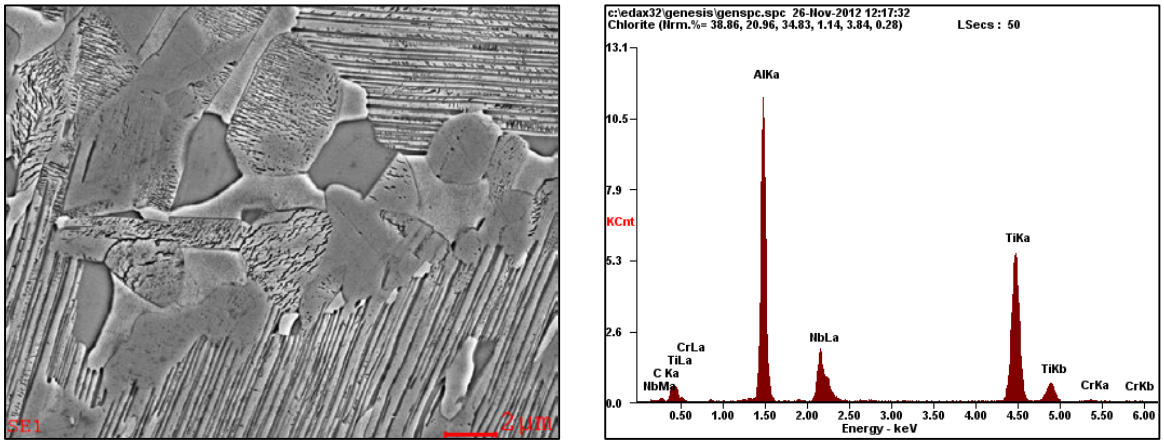

Fig. 9. Microstructure of basic material

Table 5.1 shows us the weight percentage and atomic percentage representations of the elements in this alloy.

***Tab. 5.1** Wt% and At% of the elements*

ELEMENT	***WT %***	***AT %***
AlK	**31.02**	**44.93**
TiK	**51.59**	**42.10**
NbL	14.79	06.22
CK	01.92	06.24
CrK	00.68	00.51

It was decided to use a multipoint chemical analysis for more accurate results, which indicates the representation of elements in certain phases (Fig. 10).

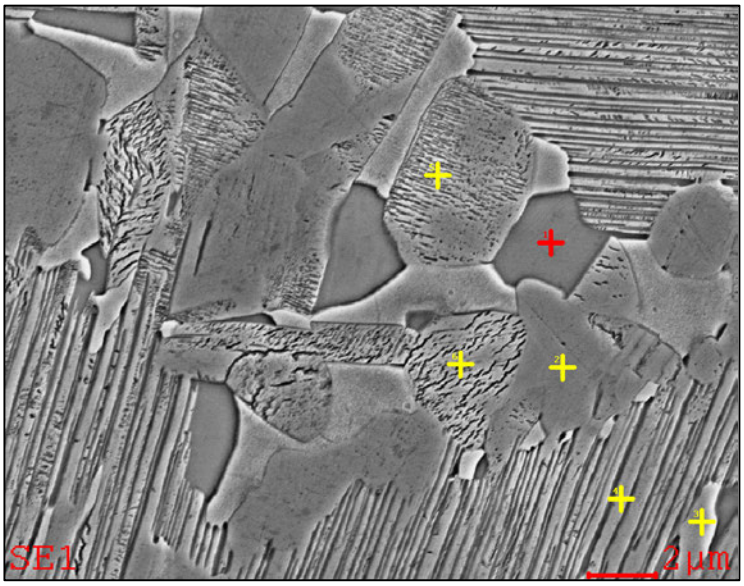

Fig. 10. Multipoint chemical analysis

Tab. 5.2 *Weight percentage of the elements in the alloy*

PLACE	C [%]	O [%]	AL [%]	NB[%]	TI [%]	CR [%]	NI [%]
point 1	1,79	1,36	**26,07**	13,94	**56,15**	0,55	0,13
point 2	1,81	1,11	**32,12**	14,72	**49,43**	0,45	0,36
point 3	2,10	1,24	**30,32**	14,46	**51,06**	0,43	0,41
point 4	1,48	1,11	**32,20**	14,78	**49,66**	0,37	0,40
point 5	2,85	1,39	**26,32**	15,94	**51,27**	1,35	0,88
point 6	2,34	1,19	**31,86**	14,43	**49,44**	0,40	0,34

Tab. 5.3 *Atomic representation of the elements in the alloy*

PLACE	C [%]	O [%]	AL [%]	NB [%]	TI [%]	CR [%]	NI [%]
point 1	5,89	3,36	**38,10**	5,92	**46,23**	0,42	0,09
point 2	5,77	2,65	**45,51**	6,06	**39,45**	0,33	0,24
point 3	6,69	2,96	**43,02**	5,96	**40,80**	0,31	0,26
point 4	4,74	2,68	**45,98**	6,13	**39,94**	0,27	0,26
point 5	9,19	3,37	**37,76**	6,64	**41,44**	1,01	0,58
point 6	7,35	2,80	**44,55**	5,86	**38,93**	0,29	0,22

5.2 Melting

Results of remelting are shown in the following figures:

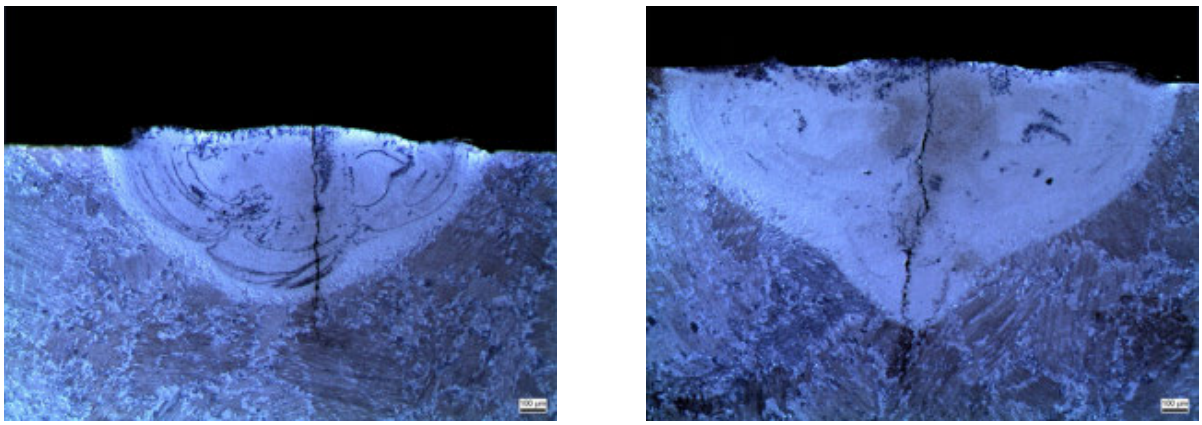

Fig. 11. Sample 1.1. Diameter = 1 mm, speed = 1000 mm/min, gas flow = 20 l/min, power = 1 kW

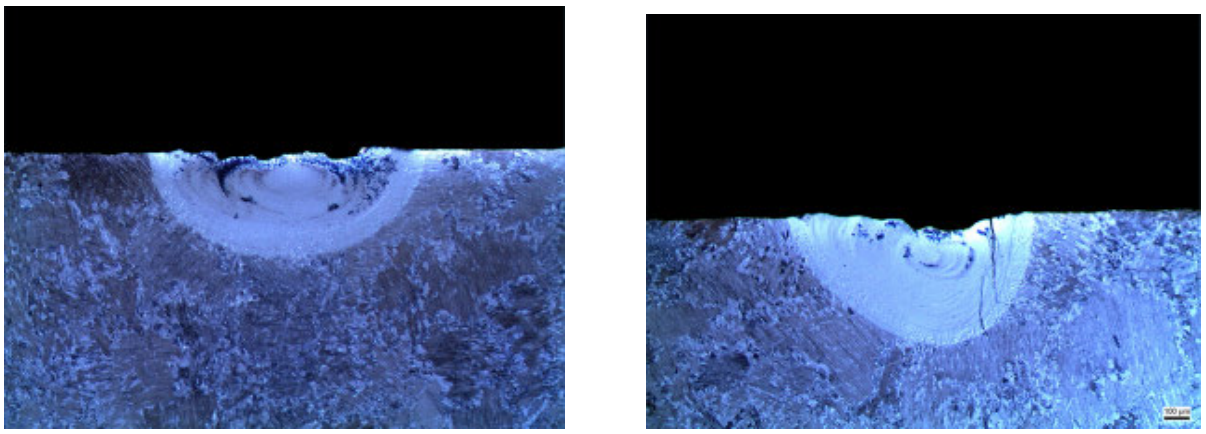

Fig. 12. Sample 1.2. Diameter = 1 mm, speed = 1000 mm/min, gas flow = 40 l/min, power = 1 kW

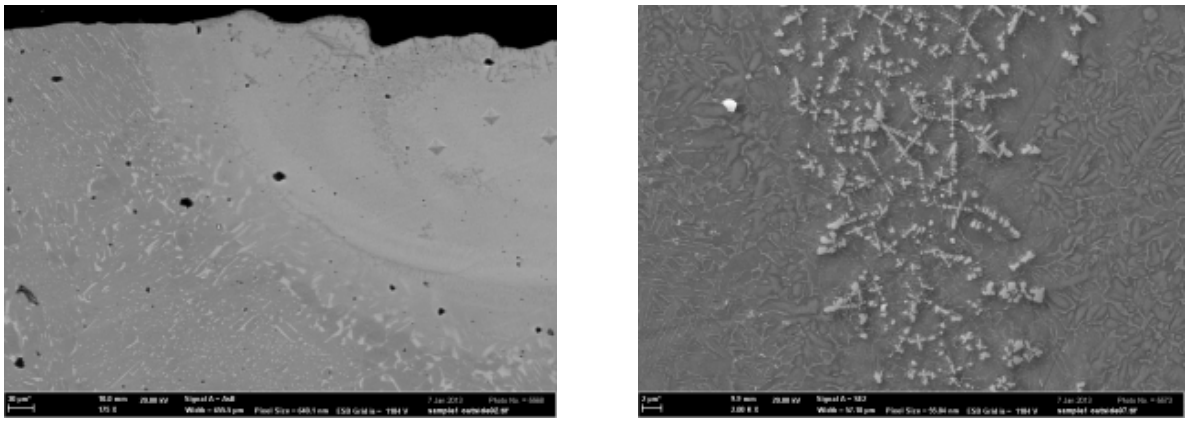

Fig. 13. Three areas of material after melting (a) and formed dendrites (b)

In Fig. 13(a) we can see changes to the original structure which occurred during melting. These correspond to a coarsening of the structure in the remelted zone. We should see two phases similar as those before melting - near γ-TiAl and α_2-Ti_3Al.

However, this is only seen in one. This is due to the fact that there was a very rapid cooling and the phases were mixed in the process of melting. The phases had not enough time for separation which is due to fast cooling. This effect occurred in each experiment. Dendrites as shown in Fig. 13(b) occur below the surface and also inside the molten zone. These dendrites were displaced from the surface due to dynamic effects, which are exerted during melting.

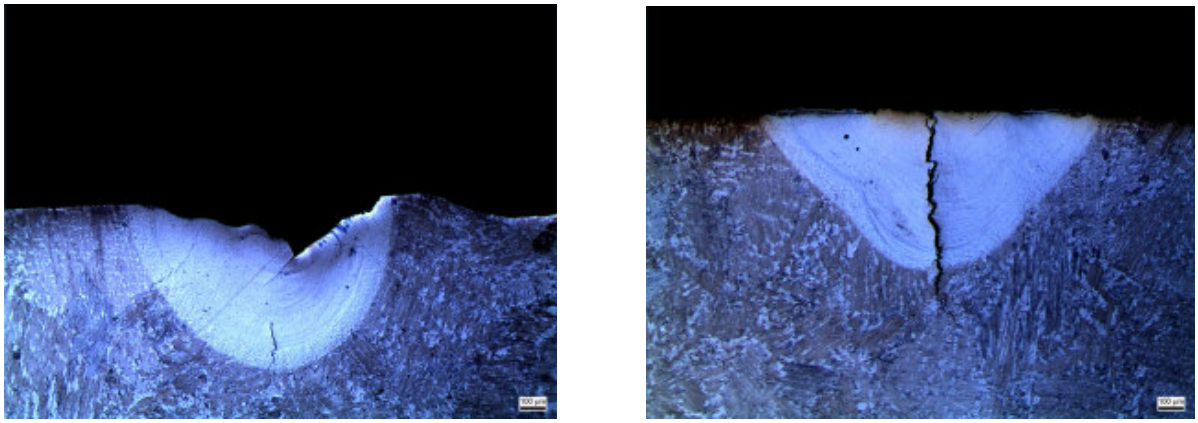

Fig. 14. Sample 2.1. Diameter = 1 mm, speed = 1000 mm/min, gas flow = 30 l/min, power = 1 kW

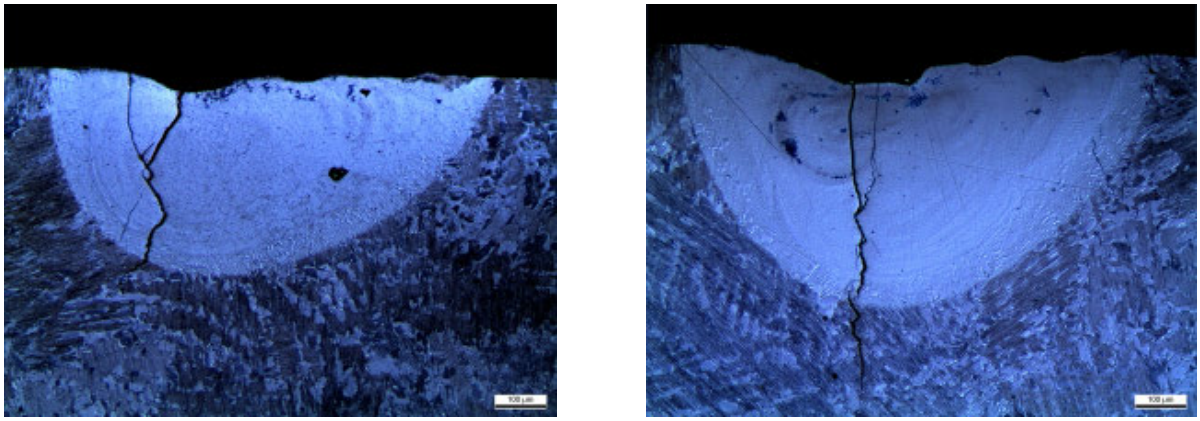

Fig. 15.Sample 2.2. Diameter = 1 mm, speed = 1500 mm/min, gas flow= 40 l/min, power=1kW

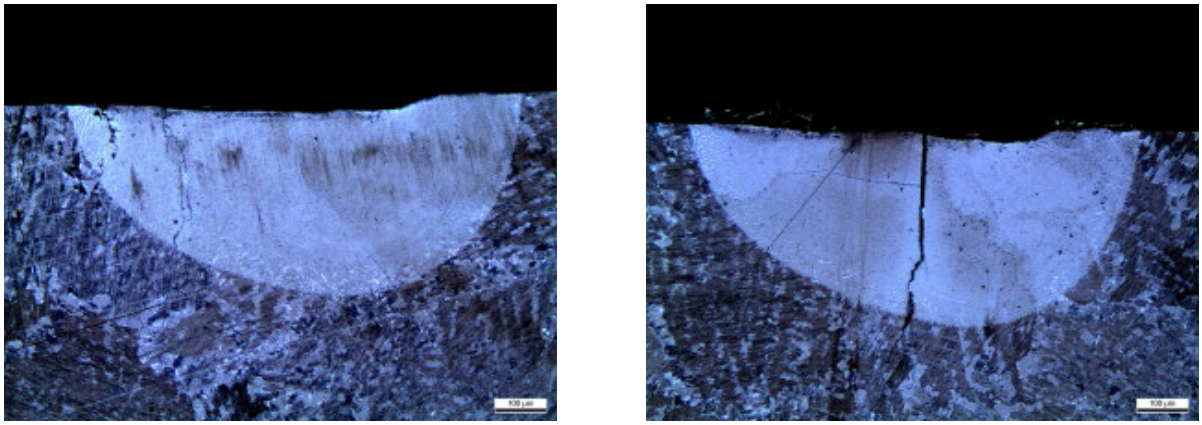

Fig. 16. Sample 3.1. Diameter = 1 mm, speed = 1500 mm/min, gas flow = 40 l/min, power = 1 kW

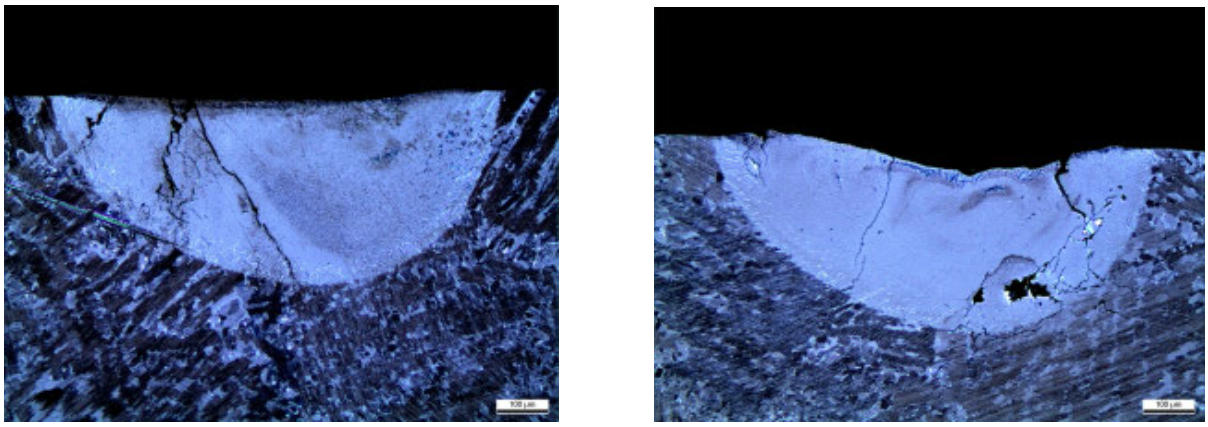

Fig. 17.Sample 3.2. Diameter = 1mm, speed = 1500mm/min, gas flow = 40 l/min, power =1kW

Fig. 18.Created dendrites

The formed nitrides are fairly visible in Fig. 18, which also shows a continuous surface layer of nitrides. In consideration of the high content of titanium and increase of nitrogen, created nitrides are probably TiN.

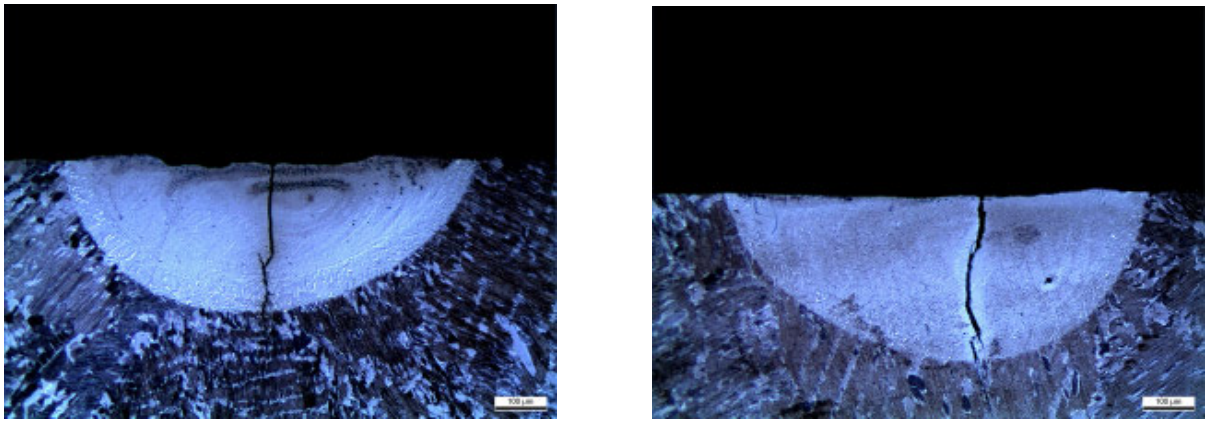

Fig. 19.Sample 4.1. Diameter =1mm, speed = 2000 mm/min, gas flow = 40 l/min, power =1kW

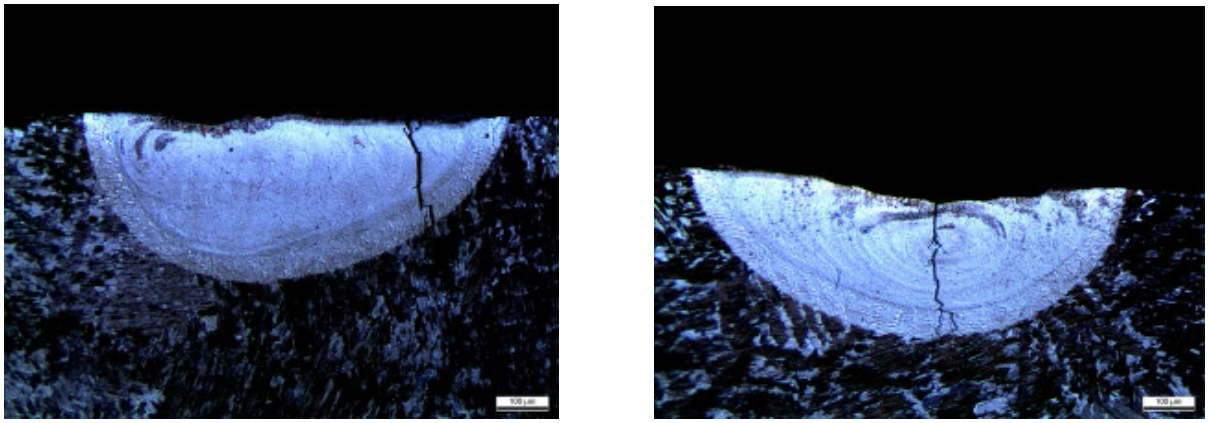

Fig. 20.Sample 4.2. Diameter = 1mm, speed = 2000mm/min, gas flow = 40 l/min, power =1kW

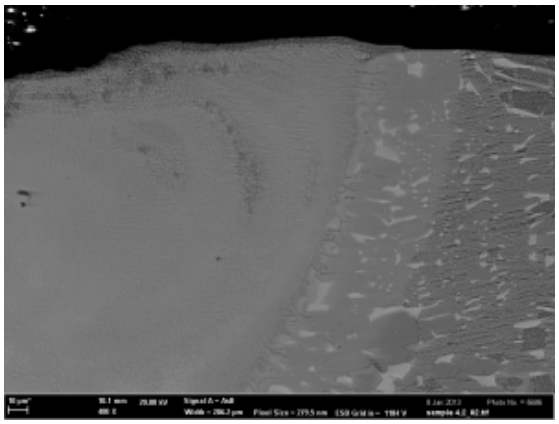

Fig. 21. Three areas of material after melting

Here we can notice what the differences are between all incurred areas. The middle zone is semi-liquid; so-called „mushy" zone. The zone is also influenced, but the material is only partially melted. Changes of the basic structure shown are not so big. In Fig. 22 we can see the mapping chemical analysis of sample No. 4. Here we can clearly observe that the nitrides created are those of titanium. Aluminum and niobium were essentially displaced due to the reaction.

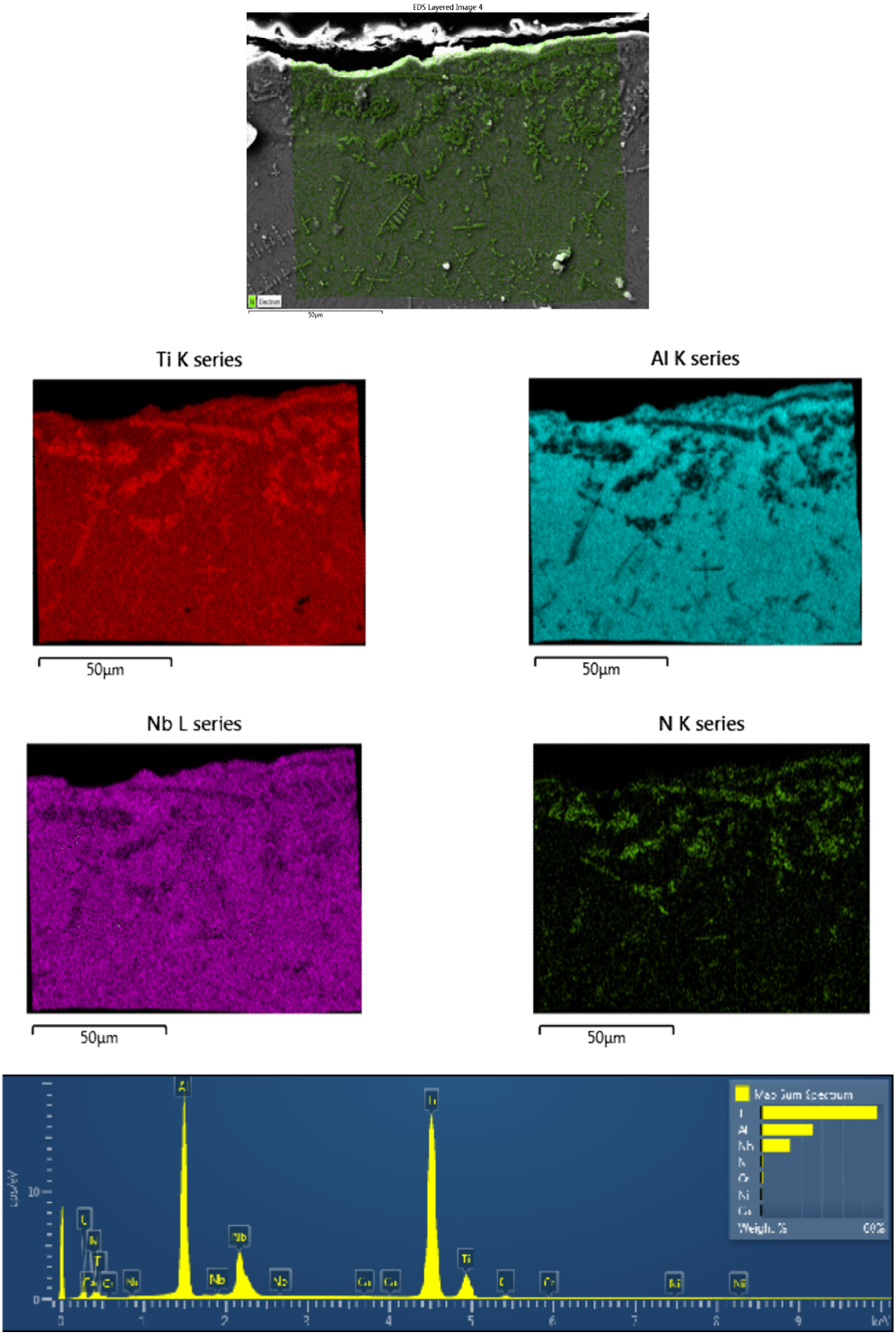

Fig. 22.Mapping chemical analysis

The increase in the content of nitrogen, which was not present here before, is also observed.

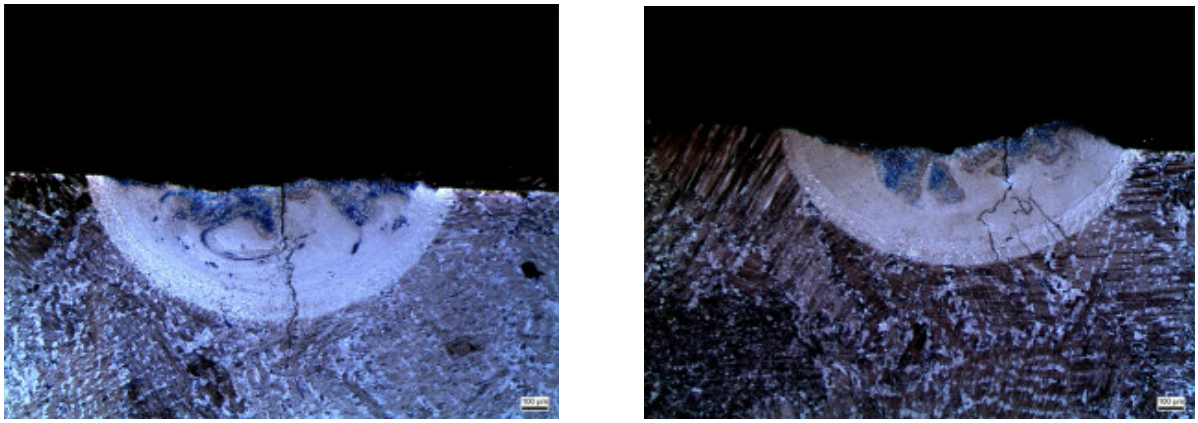

Fig. 23.Sample 5.1. Diameter=1,5 mm, speed=1000 mm/min,gas flow = 40 l/min, power=1kW

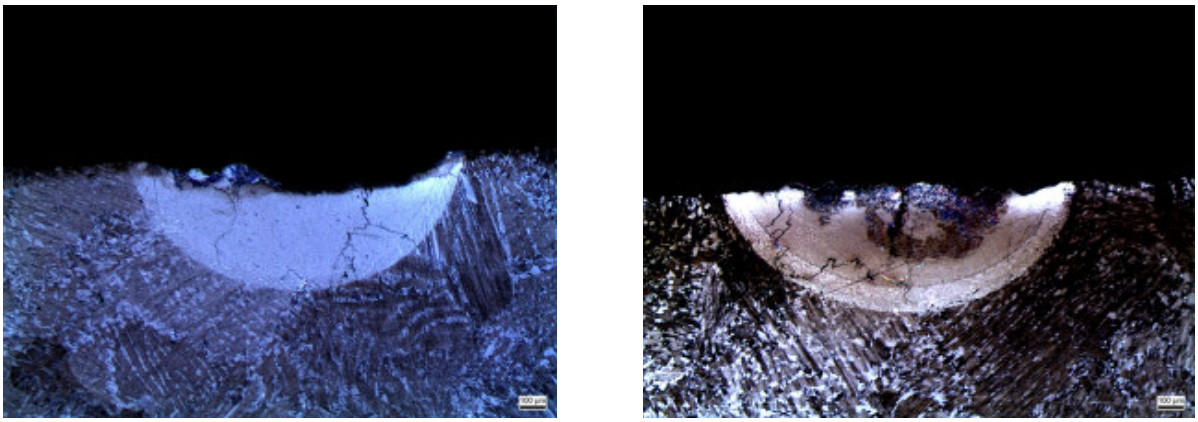

Fig. 24.Sample 5.2. Diameter =1,5mm, speed=1000 mm/min, gas flow = 40 l/min, power=1kW

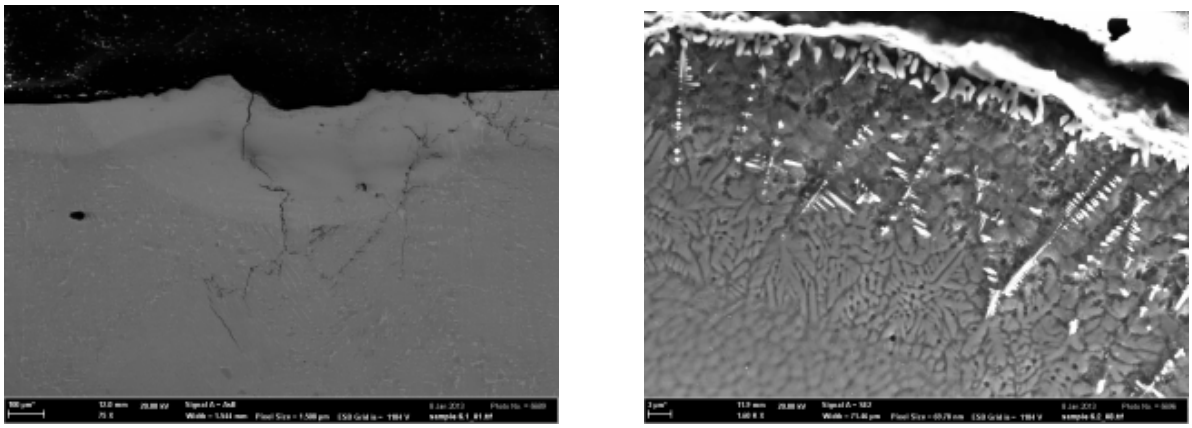

Fig. 25.Sample 6.1.and 6.2. Diameter = 1,5 mm, speed = 1500 mm/min, gas flow = 40 l/min, power = 1 kW

Clear identification of microstructure features was not possible on the optical microscope. In the scanning electron microscope pictures we can see that the sample fractured in the same way as the samples before. The layer of nitrides on the surface was also created on these specimens.

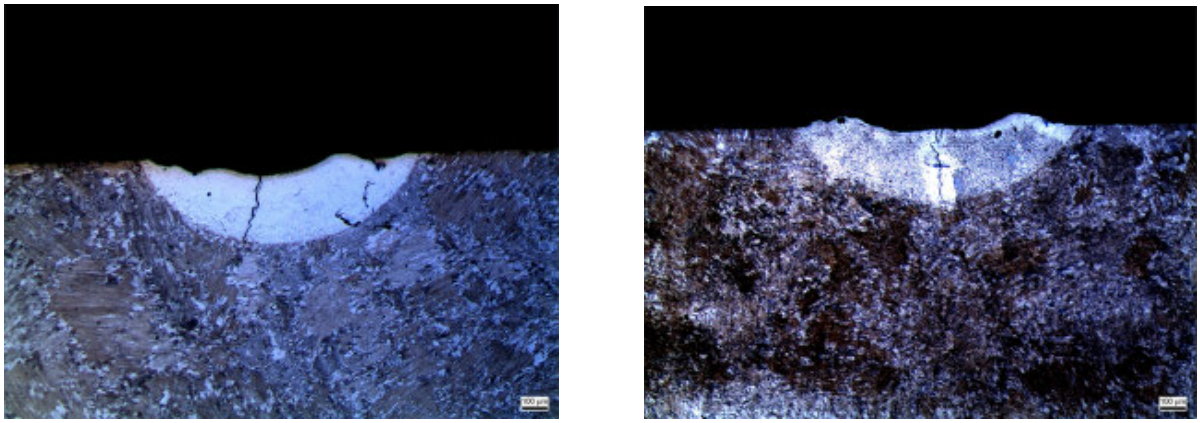

Fig. 26.Sample 7.1. Diameter=1,5 mm, speed=2000 mm/min, gas flow = 40 l/min, power=1kW

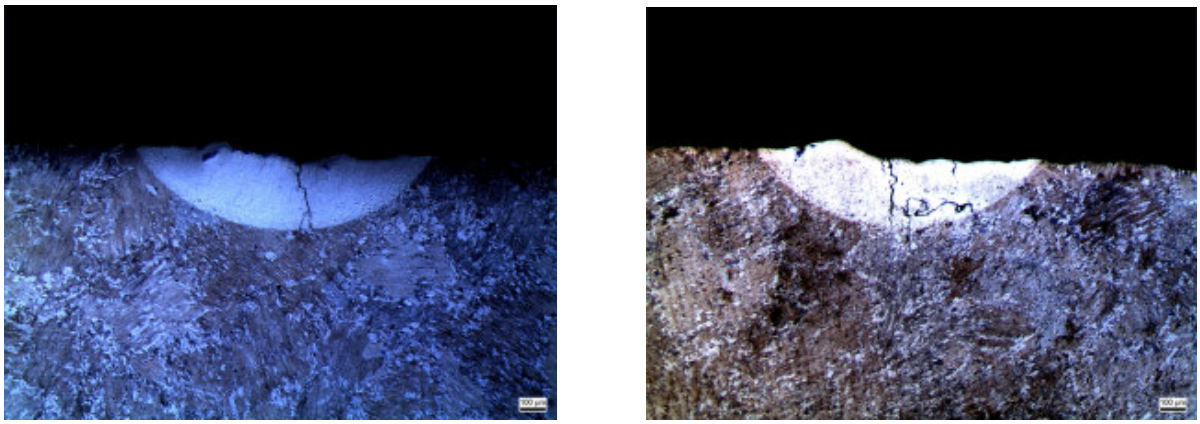

Fig. 27.Sample 7.2. Diameter=1,5 mm, speed=2000 mm/min, gas flow = 40 l/min, power=1kW

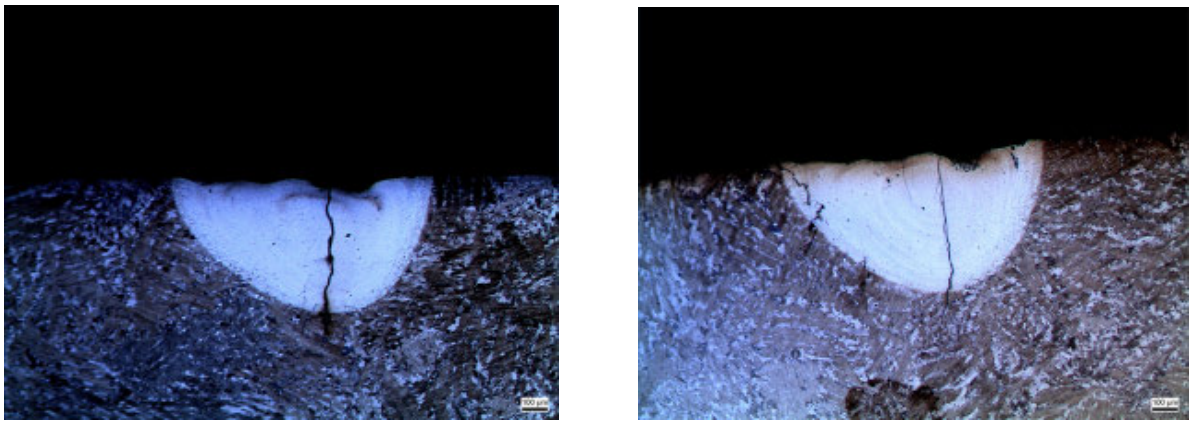

Fig. 28.Sample 8.1. Diameter = 1 mm, speed = 1000 mm/min, gas = 40 l/min, power = 1 kW

Fig. 29 is the mapping chemical analysis of sample No. 7, which shows precipitated nitrides of titanium.

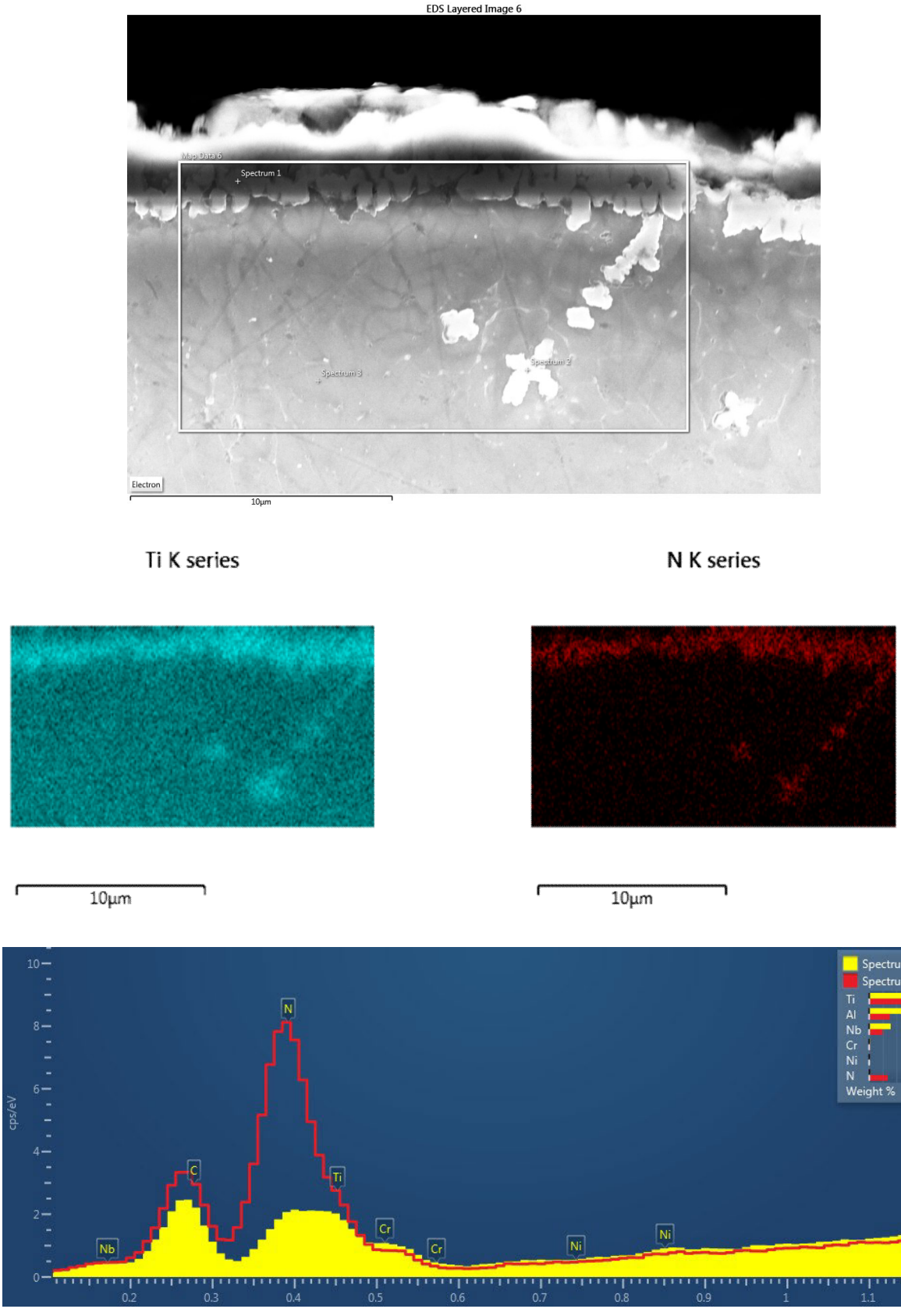

Fig. 29.Mapping chemical analysis of sample No. 7

For the two following samples the “pulsing” method was used. In this method, the power of ray was periodically changed from 100% to 25% as showed in Fig. 30:

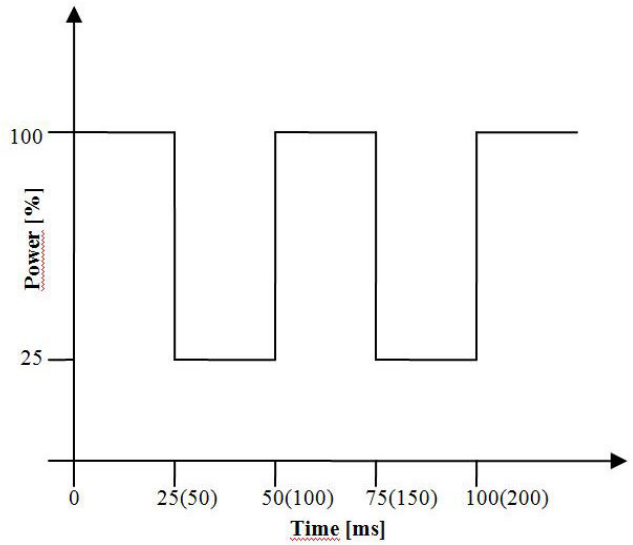

Fig. 30. Diagram of pulsing

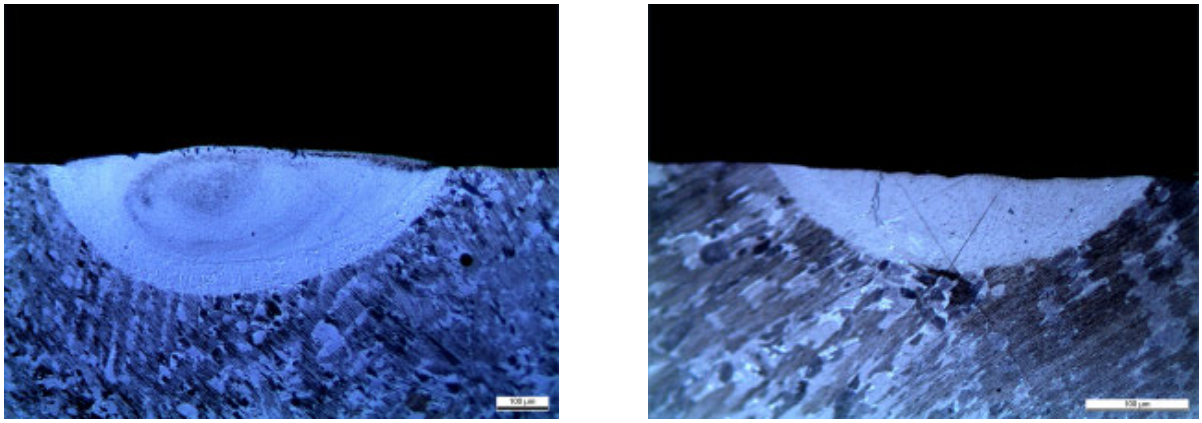

Fig. 31.Sample 8.2. Diameter = 1 mm, speed = 1000 mm/min, gas flow = 40 l/min, power = 1 kW, span = 50 ms

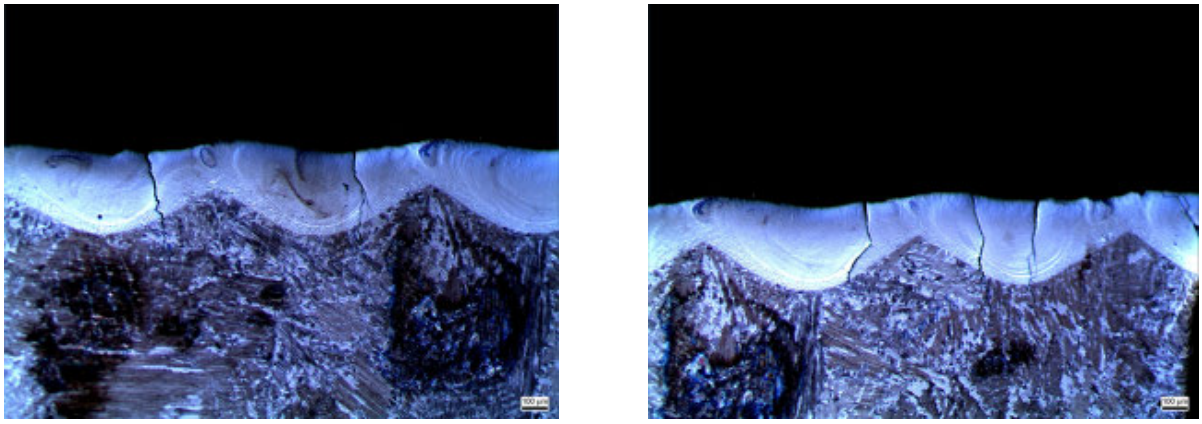

Fig. 32. Sample 9.1. Diameter = 1 mm, speed = 1000 mm/min, gas flow = 40 l/min, power = 1 kW, span = 25 ms

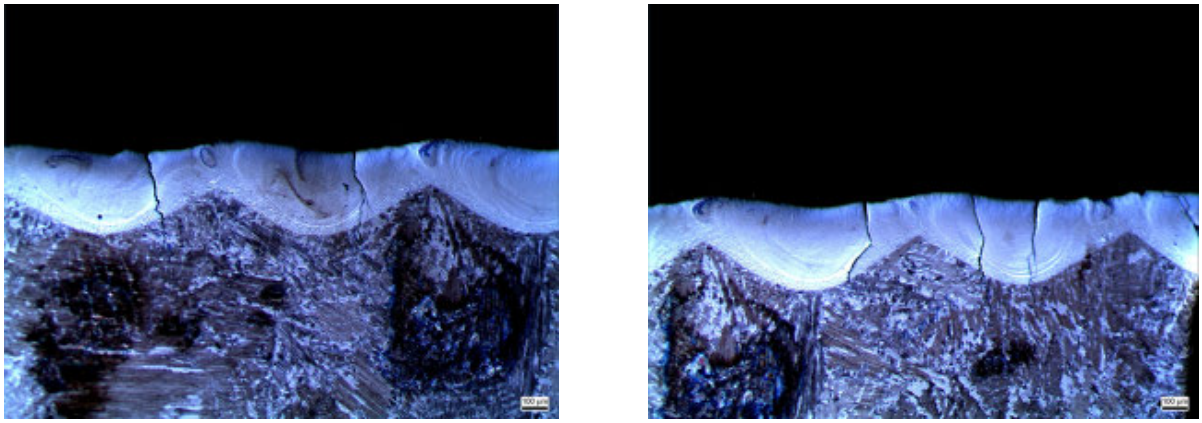

Fig. 33.Sample 9.1. Diameter = 1 mm, speed = 1000 mm/min, gas flow = 40 l/min, power = 1 kW, span = 25 ms

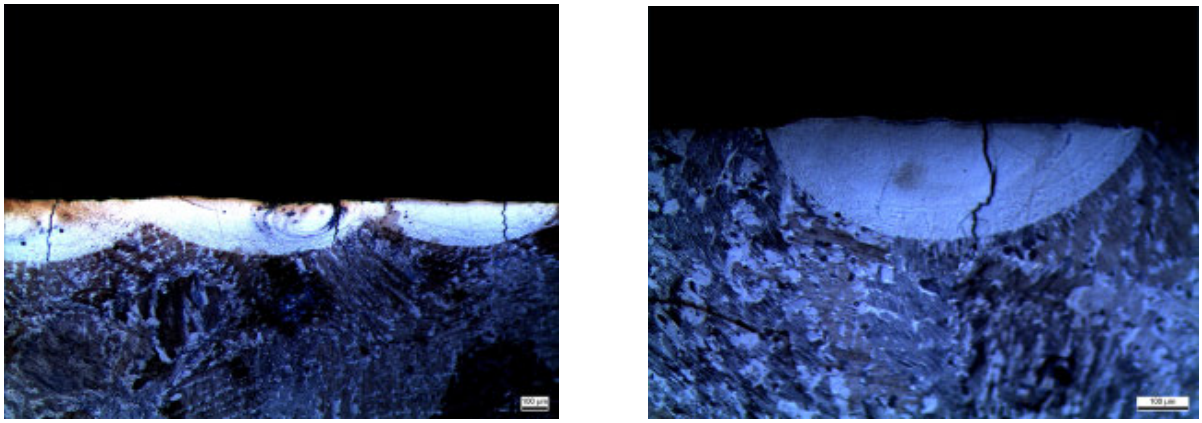

Fig. 34.Sample 9.1. Diameter = 1 mm, speed = 1000 mm/min, gas flow = 40 l/min, power = 1 kW, span = 25 ms

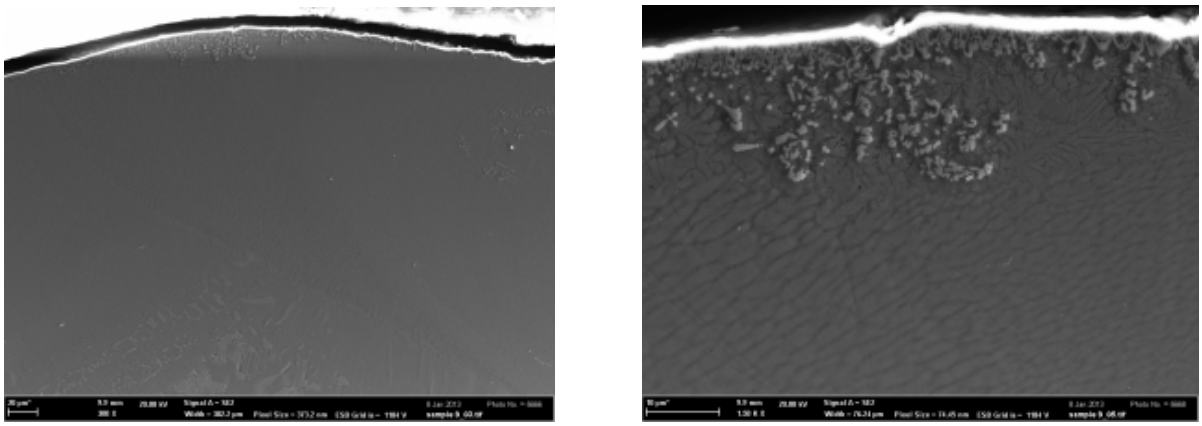

Fig. 35.Pulsing, situation - 25% of power of ray

We found that one of the two possibilities was represented here – in the region where the beam power is 25% of the total strength - the material didn't crack and also melted part looks under an optical microscope acceptable.

Parameters were tested on nine samples. We can say each of these samples has the crack after melting. This crack is probably due to the presence of tensile stresses, which are present during the cooling of the material after the melting process.

We decided to try it again in another part of the sample whilst changing only one of the parameters - diameter of ray incident on remelted sample to 2 mm.

The results of beams testing are as follows:

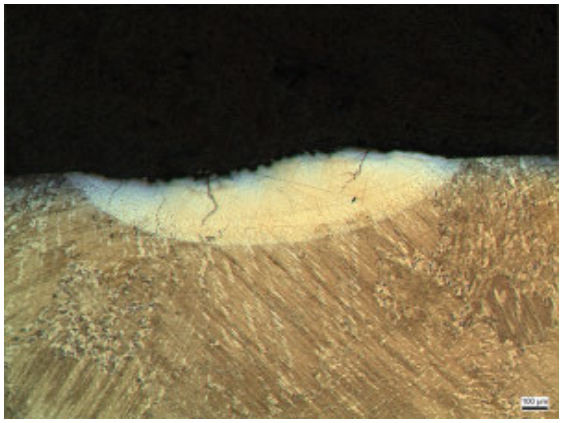

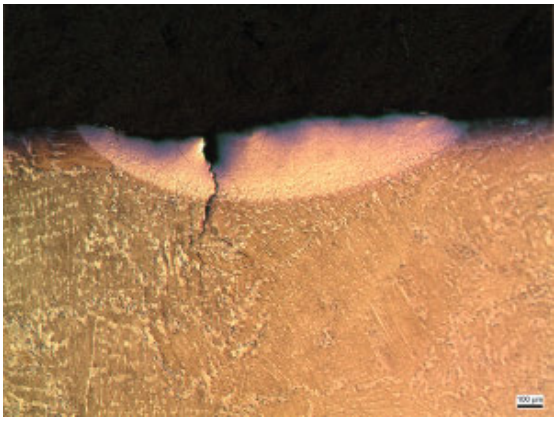

Fig. 36.Sample 10.1. Diameter = 2 mm, speed = 1000 mm/min, gas flow = 40 l/min, power = 1 kW

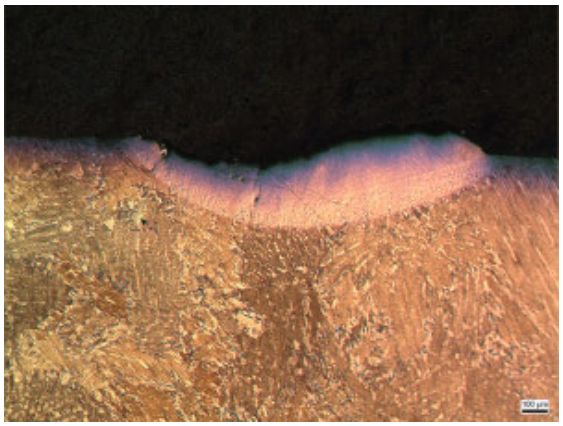

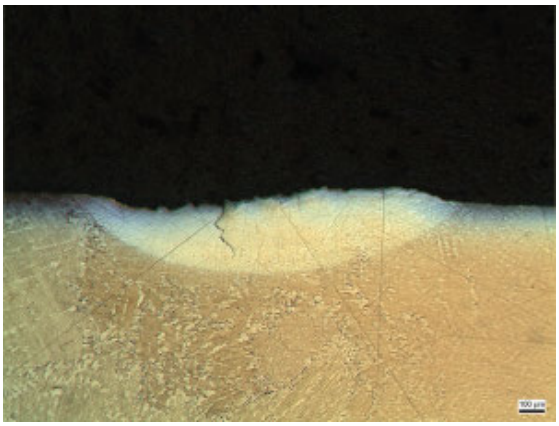

Fig. 37.Sample 10.2. Diameter = 2 mm, speed = 1000 mm/min, gas flow = 40 l/min, power = 1 kW

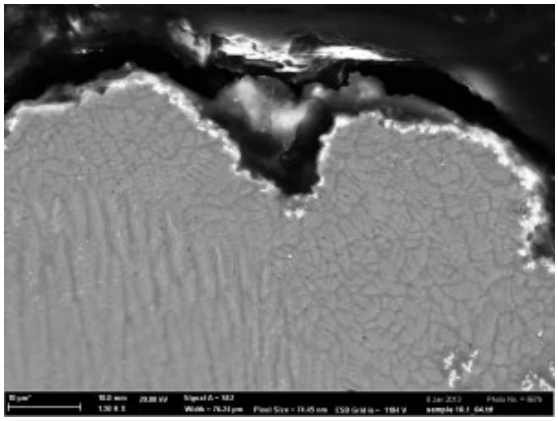

Fig. 38.Product of etching

Phase differences made evident by etching can be seen in Fig. 38. These differences are probably caused by the partial chemical heterogeneity. The two phases show to be no longer recognizable.

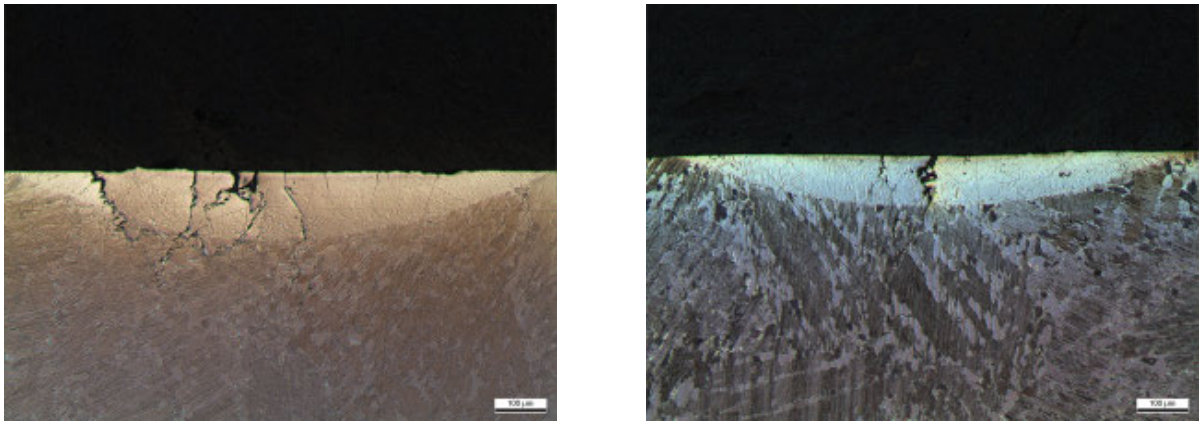

Fig. 39.Sample 11.1. Diameter = 2 mm, speed = 1500 mm/min, gas flow= 40 l/min, power = 1 kW

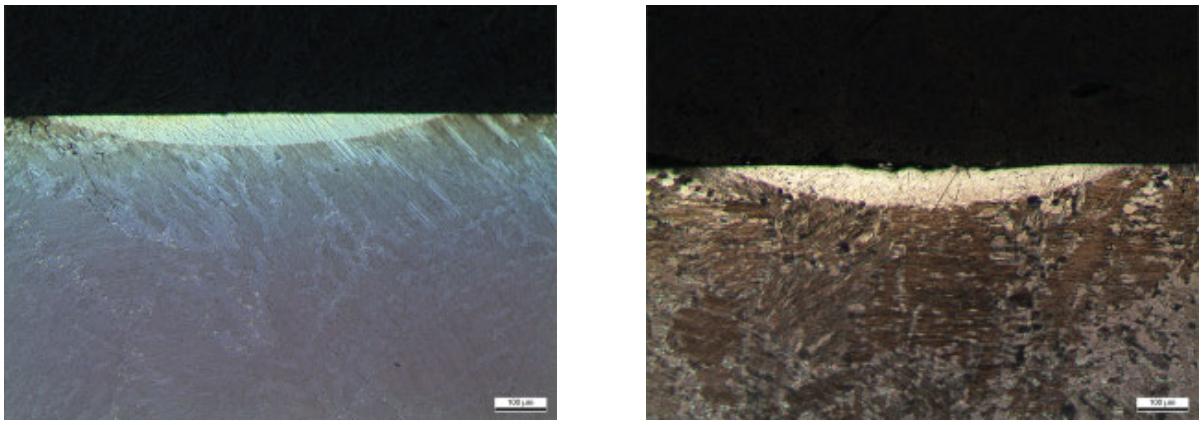

Fig. 40.Sample 11.2. Diameter = 2 mm, speed = 1500 mm/min, gas flow = 40 l/min, power = 1 kW

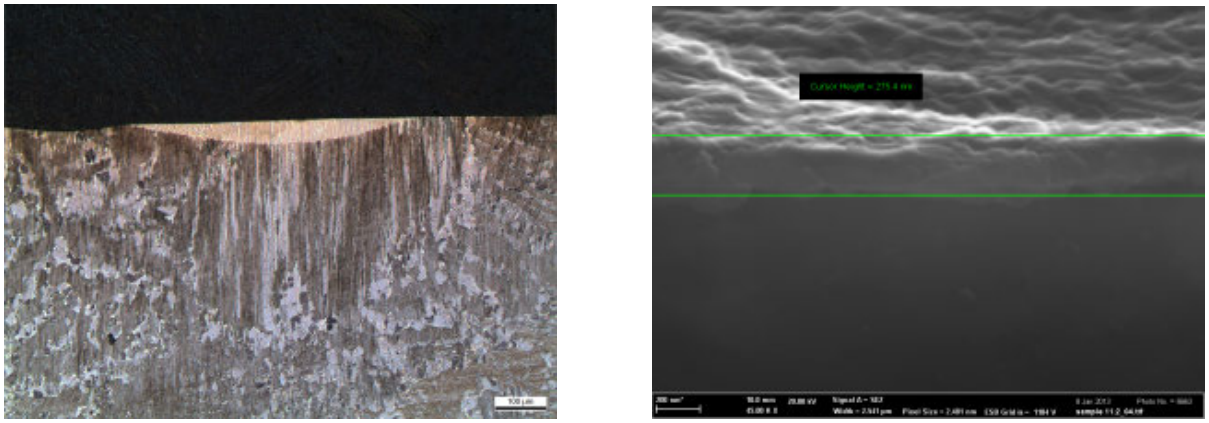

Fig. 41.Sample 12.1. Diameter = 2 mm, speed = 2000 mm/min, gas flow = 40 l/min, power = 1 kW

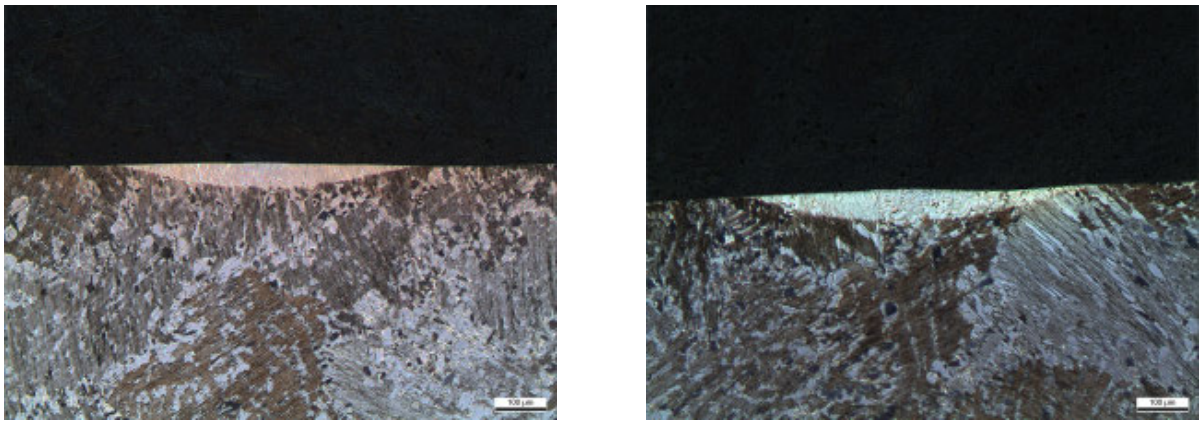

Fig. 42.Sample 12.2. Diameter = 2 mm, speed = 2000 mm/min, gas flow = 40 l/min, power = 1 kW

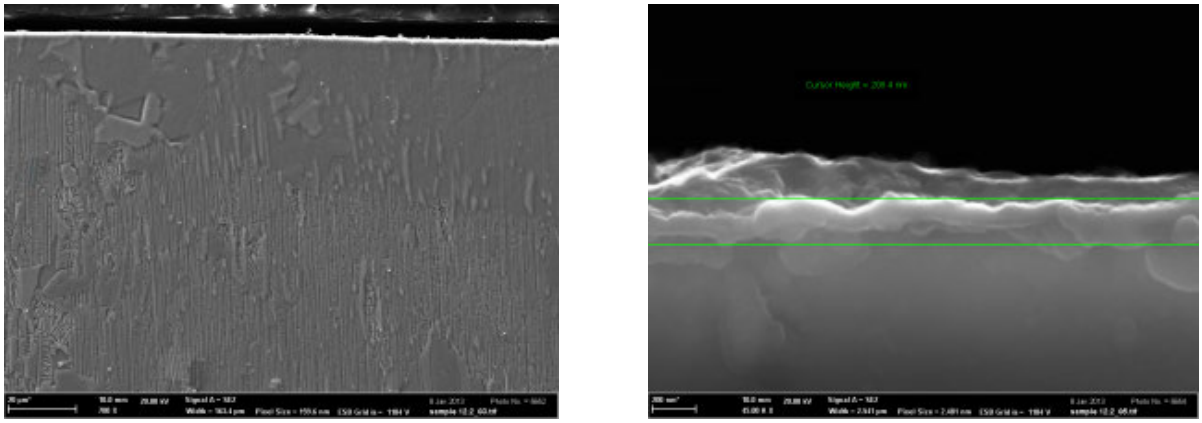

Fig. 43.Recrystallization (a) and layer of nitrides on the surface (b)

Although we avoided cracks in all of these samples, there showed to be minimal melting. The laser was at quite a distance; therefore the melting process was seen only at the center section of the beam. The diameter of the ray on the surface of samples, which made the melting, was not 2 mm but only 700 - 800 microns. In Fig. 43(a) we can see the sample had apparently not melted and likely there was only recrystallization.

A layer of nitrides was created too. We can say these parameters are acceptable in the case when we don't need to have a deep remelted and heat-affected zone. On the samples No. 13 and No. 14 we used the pulsing method, but there were no changes, due to the samples probably avoiding remelting and also recrystallization. These samples did not change their structures and the two parameters are also found to be inadequate.

The biggest problem in our experiment is cracking. The cracks occurred on all remelted samples. They are there because of the stress, which has arisen during cooling of the samples after melting process. There is a local heating and cooling which is very rapid. These cracks are fragile; we can notice that the crack doesn't effuse further into the basic material and in most of the cases they end just close to the section of melting or heat affected areas. In comparison with other samples, these cracks are very similar, so we can say these cracks are typical cracks in the melting process of the laser. The main reason of stress is very rapid heating, when the material swells its capacity, and subsequent cooling, in which the material cools down too quickly and doesn't manage to return into its original dimension.

5.2.1 Comparison our experiment with surface nitriding of Ti-6Al-4V alloy

In comparison with surface nitriding of Ti-6Al-4V alloy, where was used a high power CO_2 laser, I can say here were the same problem with cracking. In this case was nitrided layer produced by using laser power 2,5kW, a 15 mm focal length lens, a laser scanning speed900 mm/min and in a 100% nitrogen environment a flow rate 16,6 l/min. [19]

The layer of nitrides showed a golden colour and a relatively coarse surface. In the melting area perpendicular crack were observed. As well as in our case, dendrites were observed inside molten zone and in the surface nitrided layer. The content of nitrogen in the dendrites was about 10%. This fact indicated that it may be TiN (as in our case) – Fig. 44. The microhardness then grown up to 800HV. The dense dendrite areas in the layer of nitrides reflected a greater hardness compared with other regions with lower concentrations of dendrites. The high hardness near the surface was attributed to the high content of nitrogen in the surface because of any other studies. These studies had shown us that the hardness increases with increasing concentration of TiN in the nitrided layer. [19]

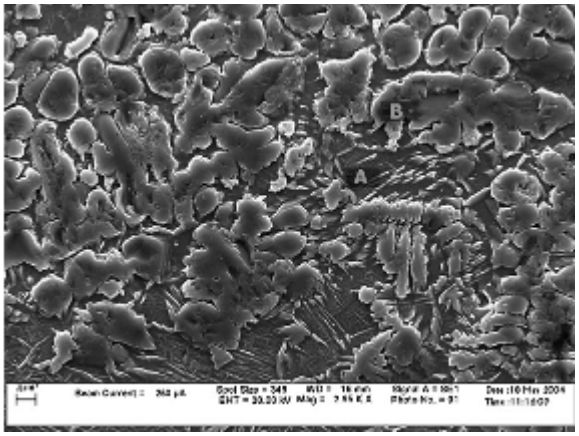

Fig. 44.SEM micrograph using back scattered electron showing the microstructure of the nitrided layer.[19]

As the biggest different between results of that melting method they saw during changes the scanning speeds. When the speed was increased, the size of nitride layer was decreased – Fig. 45. It was due to the reduction of the interaction time between the specimen and the laser beam.

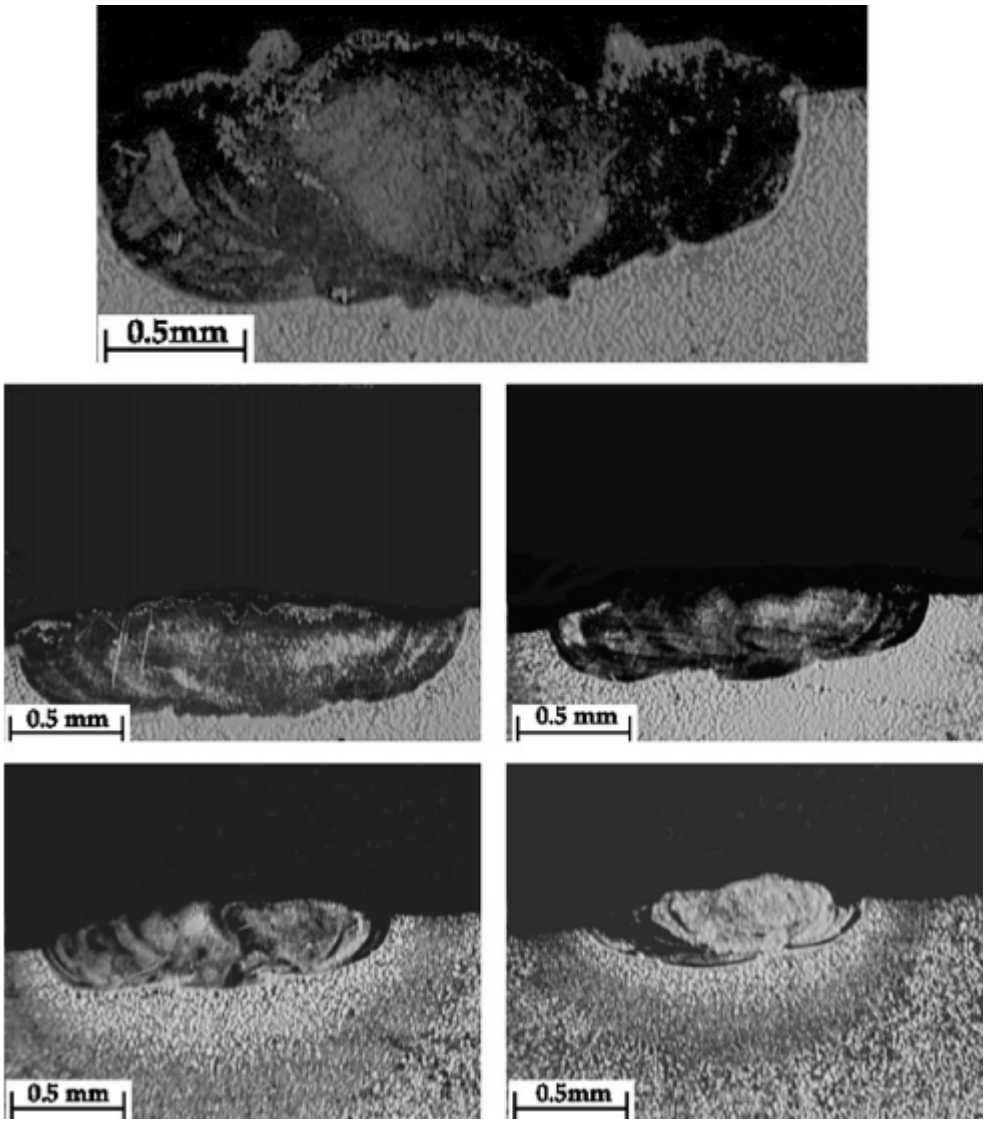

Fig. 45.Cross-section of laser tracks of Ti–6AL–4V at different traverse speeds (V): 300mm/min (a), 500mm/min (b), 800mm/min(c), 1000mm/min(d) and 1500mm/min(e) [19]

The differences between microhardness were produced also with the change of nitrogen flow rate. The best result was developed with flow rate 50 l/min – the maximum microhardness was about 724HV. This is over two times higher than the hardness of based material. [19]

Cracks had been observed specially in the nitride layers processed at slow speed and high power. For a single laser tracks, crack formation in the scan direction were occurred only for very high laser energy densities. Nevertheless, for overlapping tracks cracking was occurred in the scan direction, which could be explained by an

increase in the residual stress with each successive overlapping laser track up to maximum value. [19]

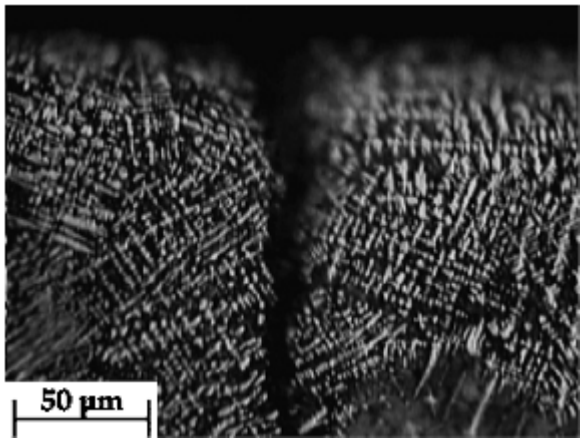

Fig. 46.Top view showing crack in some of the processed layer [19]

5.3 Microhardness

Due to the changes in the structure, we decided to test the microhardness to find out what was changed in this area. The results of the measurement of microhardness are in the table 5.4.

***Tab. 5.4** Result of microhardness*

Specimen	**Microhardness [HV]**				
-	*Position 1*	*Position 2*		*Position 3*	
1.1.	375	505	507	566	548
1.1.	372	466	528	579	608
1.2.	381	584	472	686	720
1.2.	388	580	461	640	589
2.1.	377	493	511	607	532
2.1.	422	460	630	667	683
2.2.	398	438	519	521	660
2.2.	434	449	509	607	640
3.1.	397	481	478	642	586
3.1.	378	563	480	581	668
3.2.	382	496	489	634	593
3.2.	403	461	513	683	619
4.1.	383	471	493	631	587
4.1.	389	484	495	584	658
4.2.	367	486	491	628	525
4.2.	391	483	469	609	679
5.1.	392	533	541	565	597
5.1.	393	520	542	628	567
5.2.	380	540	519	711	654
5.2.	374	514	459	563	515

6.1.	418	322	299	491	369
6.1.	426	370	296	531	521
6.2.	411	373	367	563	486
6.2.	403	424	419	590	563
7.1.	369	467	519	507	472
7.1.	366	443	472	477	429
7.2.	362	472	243	514	525
7.2.	364	478	451	519	489
8.1.	363	469	448	530	560
8.1.	358	475	434	582	591
8.2.	392	383	439	468	511
8.2.	379	443	490	576	599
9.1.	381	445	412	488	488
9.1.	376	463	408	580	480
10.1.	368	412	456	487	559
10.1.	380	528	512	509	473
10.2.	364	484	521	505	566
10.2.	401	484	476	490	512
11.1.	350	482	451	476	512
11.1.	378	531	515	505	506
11.2.	386	482	451	476	512
11.2.	368	479	405	502	515
12.1.	414	412	412	493	487
12.1.	374	399	351	362	386
12.2.	399	388	384	374	365
12.2.	414	476	408	496	502

The average value of microhardness of basic material was measured 385 HV. It is obvious that the highest microhardness was measured inside the remelted areas. On the transition section, where came through a recrystallization or only the small remelting, the measured values were lower than inside the molten area but higher than from the basic material. After look down on the result of microhardness, I consider the using Knoop methods would be more appropriate, especially because the Vickers indentation diagonal is just only about 1/3 of the length of major Knoop diagonal. Second reason for using Knoop test is that Vickers test is more sensitive to measurement errors than Knoop test and less sensitive to surface conditions. [21]

5.4 Reflectivity

An area for which the measurement was relatively safe was cropped from the sample. In the visible region the beam reflected constantly about 30%. That corresponds to the surface that can be seen - gray and unpolished - Fig. 47.

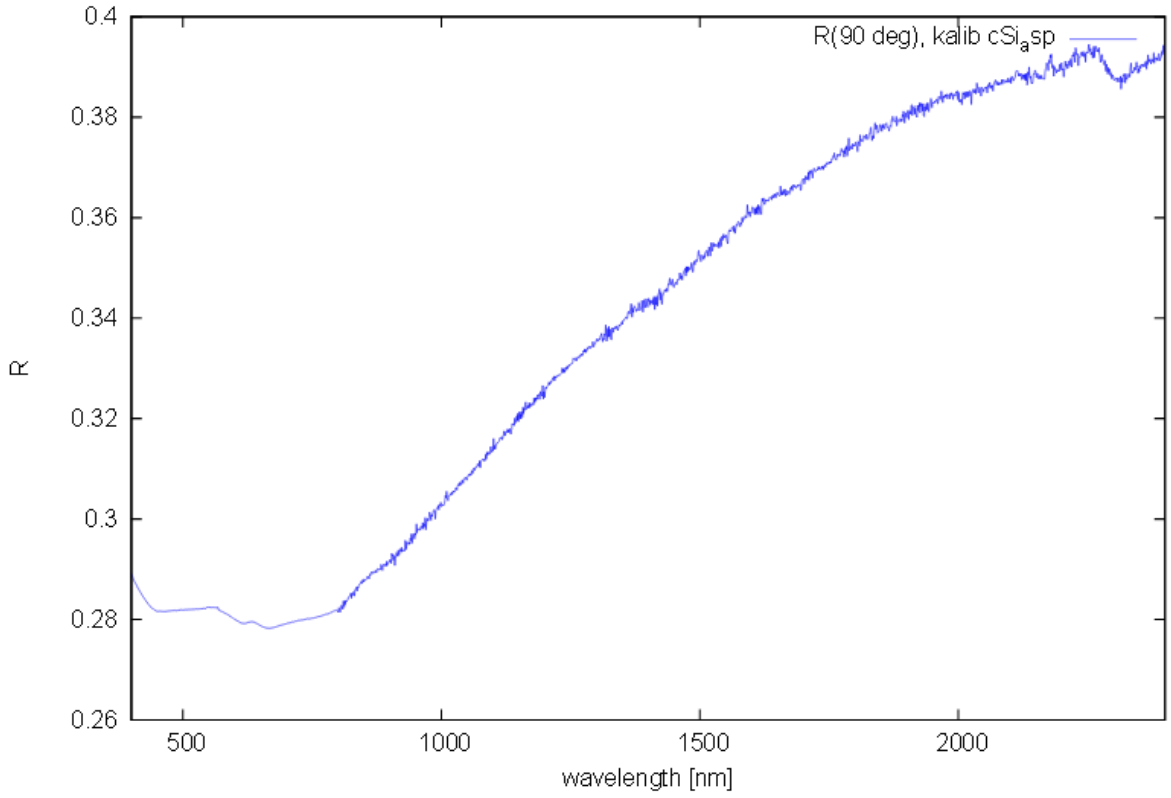

Fig. 47. Diagram of reflectivity

5.5 Oxidation process

The oxidation process did not record any large changes in the weight. It appears from this that the created layer of oxides was very small. At the moment when the samples were pressed in the bakelite resin, the layer of oxides was glued upon that resin and during the cooling process it became unstuck from the melted layer. This was due to internal stresses of the bakelite resin. It can be seen in Fig. 48 and Fig. 49.

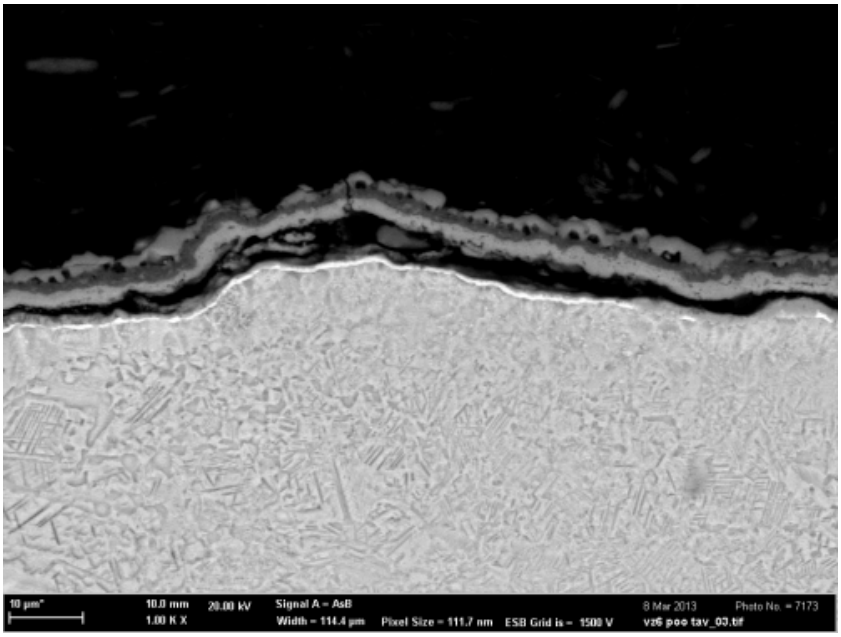

Fig. 48.The layer of oxygen unstuck from the melted layer

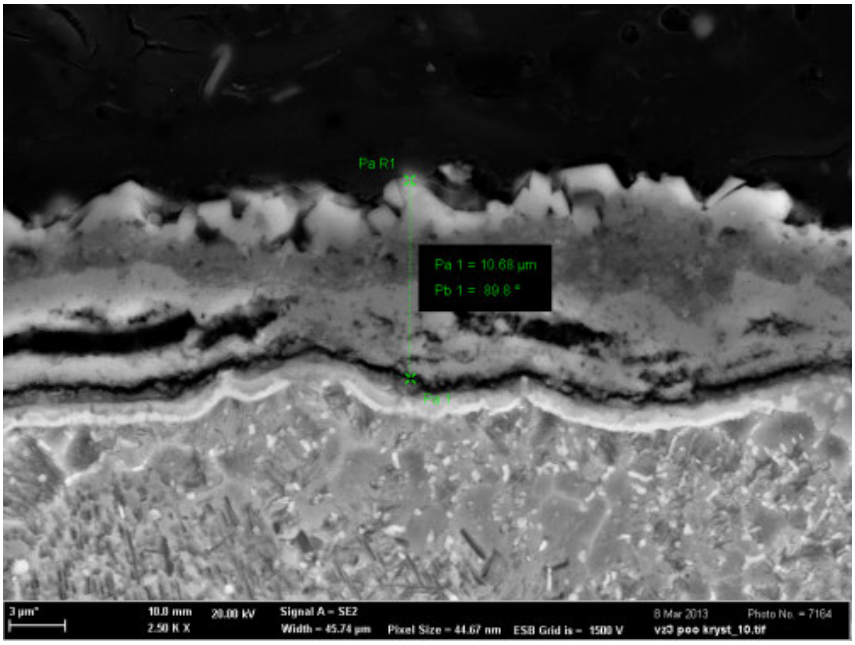

Fig. 49. The layer of oxides unstuck from the melted layer

The evidence of the existence of the created oxides can be seen in Fig. 50. The mapping analysis was carried out. The presence of oxygen is probably presented in the oxides Al_2O_3 and TiO.

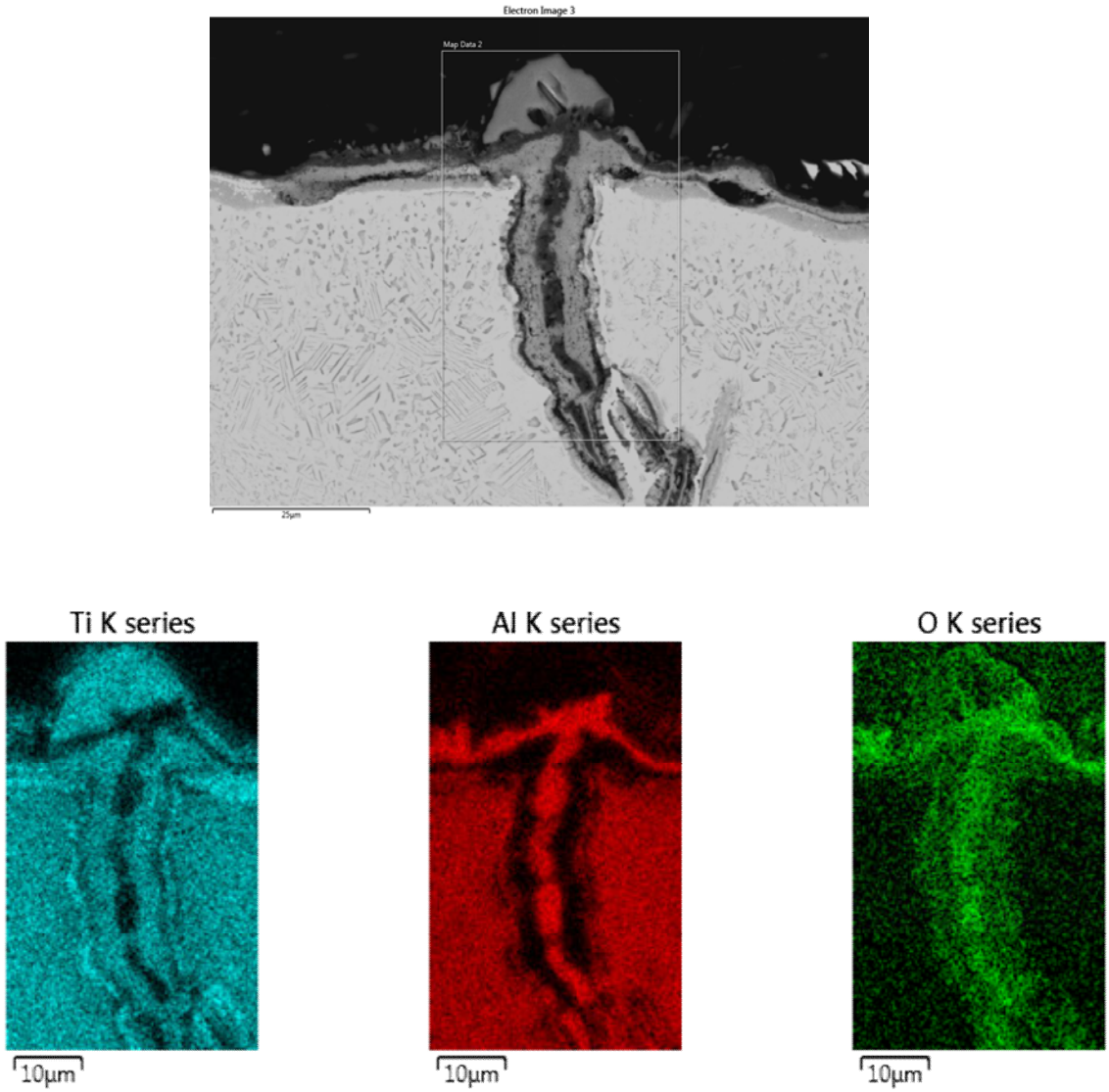

Fig. 50.Mapping analysis of sample after oxidation process

During the oxidation process a thin layer fell out from surface of melted samples. There was a difference between stress in the basic material and the oxides. These small parts of oxides were also put under the scanning electron microscope for chemical analysis. We can see the presence of oxides – Fig. 51, Fig. 52.

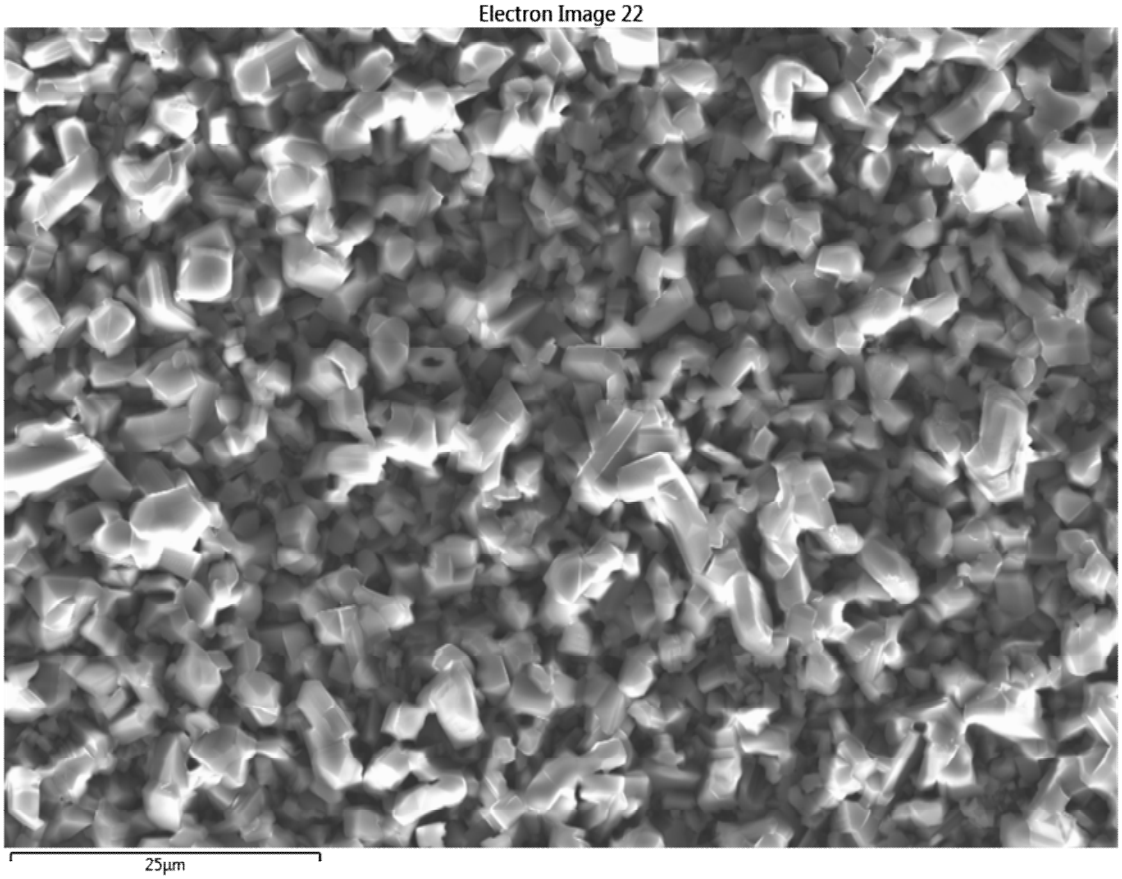

Fig. 51.Microstructure of layer of oxides

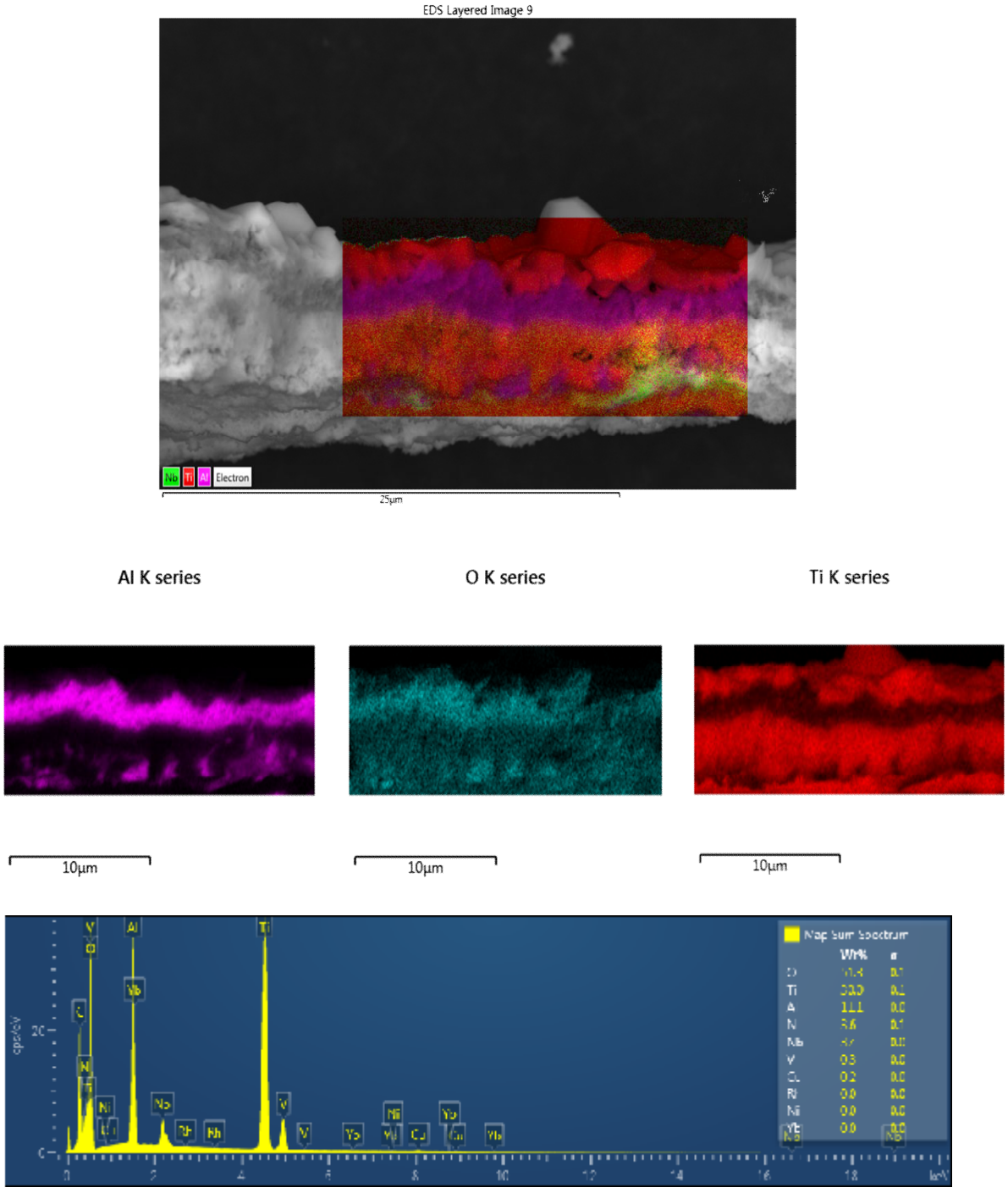

Fig. 52.Chemical analysis of layer of oxides

5.6 Three point bend test

This test was taken on the samples after isothermal oxidation at 900 °C per 100 hours. Results are shown in the Fig. 53.

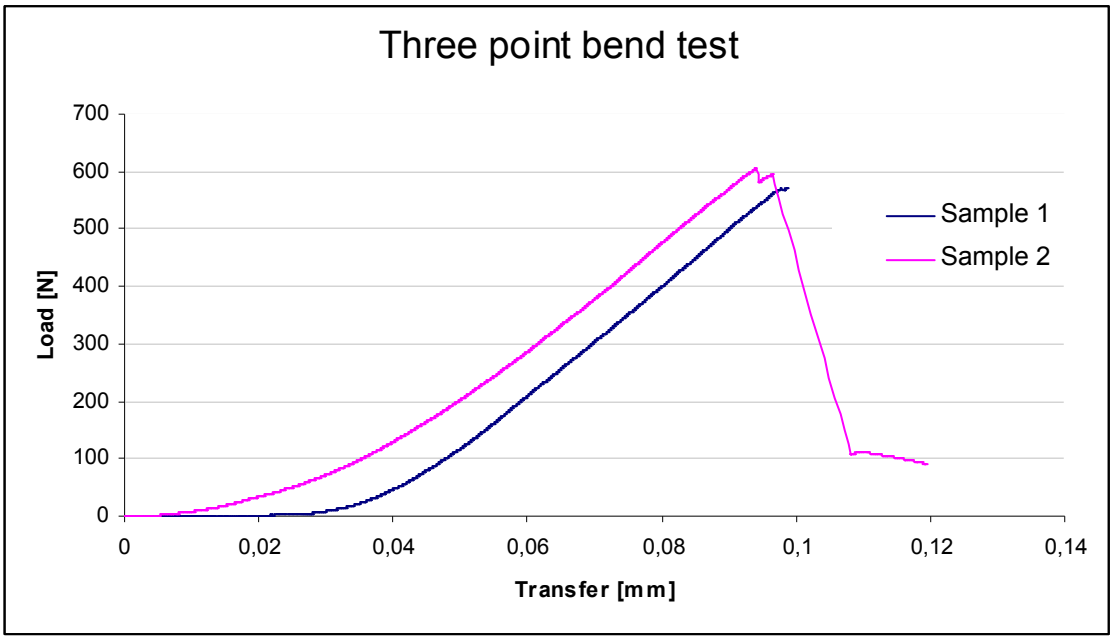

Fig. 53.Three point bend test

The effect of two peaks has arisen in consequence the resistivity of material to the diffraction. The crack stopped in this place and the crack started to spread into the material again after next straining of sample. The fission of material is not self energy. This is a typical effect for this kind of material. The diagram also indicates the final break is displayed like a sloping line. The reason is that it is needed also energy to complete break.

The resistance to fracture for the sample No. 1 was measured 364 MPa and for the sample No. 2 it was 324 MPa. In comparison with the resistance to fracture for sample of base material after oxidation is this result very similar. It may be said the melted layer of nitrides has no major impact to the increase in resistance to fracture. The structure of the fracture surface can be seen in Fig. 54.

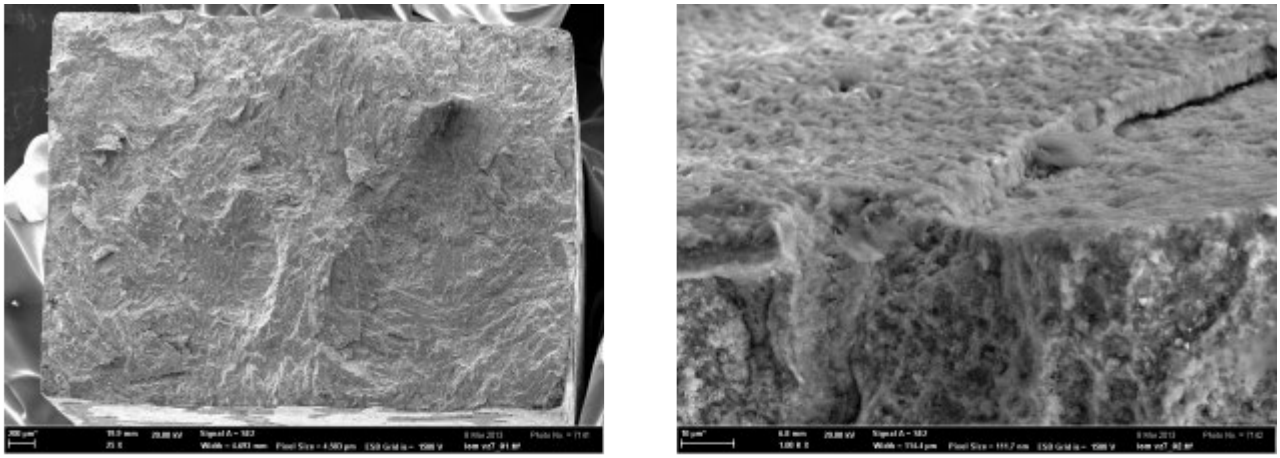

Fig. 54.The structure of the fracture surface

In Fig. 55 is shown the fracture crack.

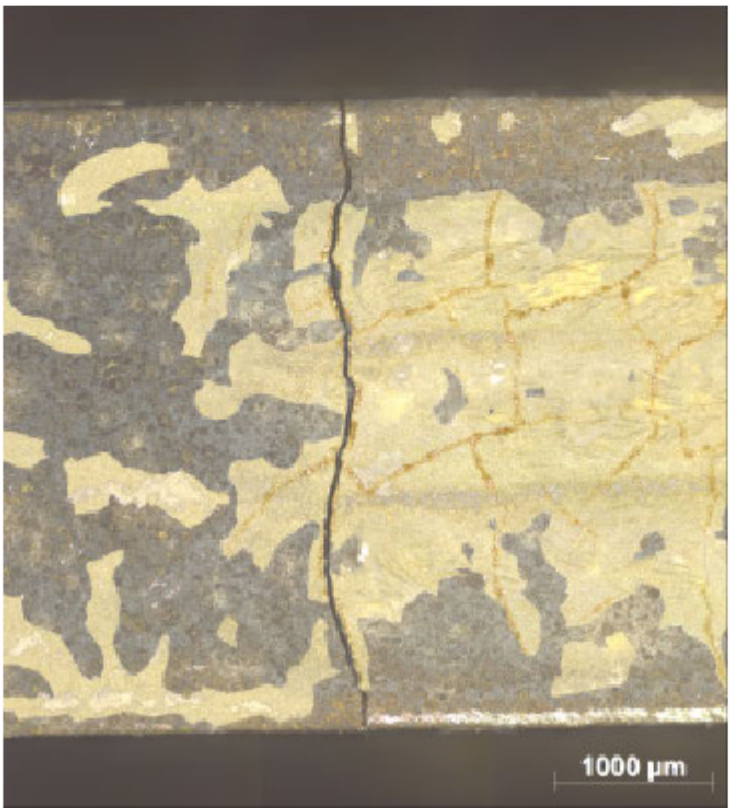

Fig. 55.Three point bend test of sample No.1

6 CONCLUSIONS

It was performed several experiments that eventually led to the proceeds of acceptable parameters for remelting of the samples. However, these results, without the appeared cracks or other defects, were only two. Other experiments have led to the cracks. Despite of these cracks, which there were practically always, we have found there the positive observation - the production of a continuous layer of nitride on the surface of the melted area. Due to the high concentration of titanium, we can say the dendrites are probably titanium nitrides. Some of these dendrites were due to dynamic effects, which were exerted during melting, moved from the surface into the remelted zone. Furthermore, coarsening of the structure in the remelted area was on the each of specimen.

In comparison with other experiment, we can say crack is probably typical problem conducting the melting process. They are there because of the stress, which has occurred on the laser tracks as a result of rapid cooling after a local heating. The material swells its capacity and subsequently, when is cooled, it has not sufficiency of time for return to its original dimension. The cracks are probably fragile, because they don't spread further into the basic material and in almost all of case end just beyond the section of melting of heat affected areas.

Acceptable conditions were found in the sample, which was used pulsing method. In the place, where a laser beam was attenuated to 25% of the total power 1kW, there have been no cracks. Second experiment with good results was with continuous laser beam in operation from a greater distance. These grateful parameters we used for our experiment.

On all of the samples was performed the measurement of microhardness. Since it is not clearly to see the difference in the microhardness of the remelted areas, I suppose the using the Knoop hardness test would be more appropriate.

These samples were inserted into the oven for subsequent isothermal
oxidation process. The thin layer of oxides fell out during the cooling process in the furnace due to stress in base material. The microstructure of these oxides has shown us probably the types of oxides TiO and Al_2O_3. It is not possible to specify it more accurately. These oxides, which have stayed on the samples, became unstuck from melted layer of the samples after the heating in bakelite resin due to internal stresses in this resin. The oxidation affected the fracture toughness. The material became be more fragile. The difference between values of resistance to the fracture for sample with oxidation and without that process is about 400 MPa.

Reflectivity of the used material corresponded to the appearance of the surface – gray and unpolished. It was reflected constantly about 30% in the visible region of the beam.

The fracture of samples after the three point bend test was cleavage fracture. The material is very fragile in basic state. Due to cracks created during the melting process there was larger stress, and the material was more susceptible to crack in the three point bend test. The resistance of base material without oxidation is 766

MPa and after the oxidation process about 330 MPa. The resistance to the fracture was reduced to 324 MPa and 364 MPa due to oxidation. The conclusion of the resistance to fracture is therefore the melted layer of nitrides has no major impact to the increase in resistance to fracture.

7 REFERENCES

[1] ION, John C. *Laser Processing of Engineering Materials: Principles, Procedure and Industrial Application*. Oxford, Elsevier – Butterworth Heinemann, 2005. Available on the website: http://books.google.com.mt/books?id=eV7o7F2MYUUC&printsec=frontcover&hl=cs#v=onepage&q&f=false

[2] T. N. BAKER, *Laser surface modification of titanium alloys*, Glasgow, The University of Strathclyde, 2010, p. 398-399

[3] INKCUPS NOW: Laser Technology. *Carbone Dioxide (CO2) and ND YAG Laser Systems* [online]. [cit. 2013-01-13]. Available on the website: http://www.inkcups.com/articles/co2-and-yag-laser-technology/Default.aspx

[4] INSTITUTE FOR MATERIALS RESEARCH. *Encyclopedia of Aerospace Engineering: TiAl Intermetallics*. Geesthacht, Germany: GKSS Research Centre, Published Online: 15th of December 2010. Available on the website: http://onlinelibrary.wiley.com/doi/10.1002/9780470686652.eae215/abstrakt

[5] AMT - Advanced Materials Technology: Materials - Titanium intermetallic. [online]. [cit. 2013-01-06]. Available on the website: http://amt-advanced-materials-technology.com/materials/titanium-intermetallic/

[6] KÁRNÍK, Tomáš, KURSA Miroslav, KRYBUS Kamil. Characteristics of Intermetallics TiAl. In: Metal2011 [online] 2011 [cit. 2012-04-03]. Available on the website: http://www.metal2011.com/data/metal2000/sbornik/papers/615.pdf

[7] SMÍŠEK, Vítězslav, KURSA Miroslav. *Vliv směrové krystalizace na mikrostrukturu slitiny Ti-46Al-5Nb-1W* [*Effect of the directional crystallization on the microstructure of alloy Ti-46Al-5Nb-1W*]. In: Metal2012 [online]. 26. 5. 2005 [cit. 2013-01-14]. Available on the website: www.metal2012.com/files/proceedings/metal_05/papers/99.pdf

[8] ZEMČÍK, Ladislav; DLOUHÝ, Antonín a UMSHAUS, Josef. *Odlévání turbínových kol turbodmychadel ze slitin TiAl* [*Casting turbine wheel of turbocharger of TiAl alloys*]. In : *Slévárenství* [*Founding*]*. LVI .* [September-October] 2008, p. 417-421.

[9] Patel, C. K. N. (1964). *Continuous - Wave Laser Action on Vibrational - Rotational Transitions of CO_2*, Physical Review 136 (5A): A1187–A1193. Available on the website: http://prola.aps.org/abstract/PR/v136/i5A/pA1187_1

[10] *Surface engineering of light alloys: Aluminium, magnesium and titanium alloys*. USA: Woodhead Publishing Limited and CRC Press LLC, 2010. Edited by Hanshan Dong

[11] LASER SYSTEMS PRODUCT GROUP. *Industrial Laser Processes*: *Laser basics - Reflections on the ins and outs of lasers*, USA: AMT - The Association for Manufacturing Technology, 1998. Available on the website: https: www.amtonline.org/

[12] MAŁECKA, J., GRZESIK, W., HERNAS A., *An investigation on oxidation wear mechanisms of Ti–46Al–7Nb–0.7Cr–0.1Si–0.2Ni intermetallic-based alloys*, [cit. 2012-12-04] Elsevier Ltd, Available online 15th of September 2009, p. 263–272. Available on the website: www.sciencedirect.com

[13] Jon's Hobby Lasers: Experiments and Learning with Laser Projects in a Hobby Setting. [online]. Available on online: 20th of June, 2009 [cit. 2013-01-20]. Available on the website: http://www.jonslasers.com/co2-laser-diagrams

[14] XINHUA WU, A. HUANG, D. HU, M.H. LORETTO. *Oxidation-induced embrittlement of TiAl alloys*. Available online 23th of February 2009 [cit. 2013-01-20] Available on the website: www.sciencedirect.com

[15] FUKÁTKOVÁ, P. *Zkřehnutí TiAl intermetalik indukované oxidací povrchu*. [*Embrittlement of TiAl intermetallics induced by surface oxidation*], Brno University of Technology, Faculty of Mechanical Engineering, 2010, Supervisor of thesis: prof. Ing. Ivo Dlouhý, Csc.

[16] SCHMIEDGEN M., GRAAT P.C.J. at al. *Thin Solid Films* 415 (2002) 114. [cit. 2013-01-19] Available on the website: www.sciencedirect.com

[17] *Intermetallics Research Progress*. USA: Nova Science Publishers, Inc., 2008. Edited by Yakov N. Berdovsky, Available on the website: http://books.google.com

[18] INSTRON, The difference is measurable: Hardness [online], [cit. 2012-12-13]. Available on the website: http://www.instron.us/wa/applications/test_types/hardness/vickers.aspx

[19] ABBOUD, J.H., FIDEL, A.F., BENYOUNIS, K.Y. *Surface nitriding of Ti-6Al-4V alloy with a high power CO_2 laser*. Available online 10th of September 2007 [cit. 2013-01-25] Available on the website: www.sciencedirect.com

[20] VOICE, W.E., HENDERSON, M., SHELTON, E.F.J., *Gamma titanium aluminide, TNB*. September 2005, [cit. 2013-01-30] Available on the website: www.sciencedirect.com

[21] SURFACE ENGINEERING FORUM, Microhardness Test [online], [cit. 2012-12-13] Available on the website: http://www.gordonengland.co.uk/hardness/microhardness.htm

[22] DONACHIE, Matthew J. *Titanium: a technical guide. 2nd ed. Materials Park*: ASM International, 2004, vii, 381 s. ISBN 08-717-0686-5.

[23] TITANIUM EXPOSED: *Titanium density - the key property that gives titanium its miraculous qualities* [online]. [cit. 2014-05-05]. Available on the website: http://www.titaniumexposed.com/titanium-density.html

[24] PODRÁBSKÝ, T. *Structure and Properties of Engineering Materials*. Lecture. Brno: Brno University of Technology, 3.12.2012

[25] DAVIS, J.R. *Titanium and Titanium Alloys*. [cit. 2014-01-16] Available on the website: http://www.asminternational.org/

[26] MAŁECKA, J., W. GRZESIK and A. HERNAS. Corrosion Science: *An investigation on oxidation wear mechanisms of Ti–46Al–7Nb–0.7Cr–0.1Si–0.2Ni intermetallic-based alloys*. January 2010 [cit. 2014-05-05] Available on the website: www.sciencedirect.com

[27] WELSCH, G., R. BOYER and E. COLLINGS. *Materials properties handbook: titanium alloys*. 1994, p. 1169. [cit. 2014-05-08] Available on the website: http://www.asminternational.org/

[28] *Titanium Alloy Properties*. [online]. 25.3.2008 [cit. 2014-05-06]. Available on the website: http://www.roymech.co.uk/Useful_Tables/Matter/Titanium.html

[29] KIM, J.P., H.G. JUNG and K.Y. KIM. Surface and Coatings Technology: *Al+Y codeposition using EB-PVD method for improvement of high-temperature oxidation resistance of TiAl*. February 1999, [cit. 2014-05-08] 91–97. Available on the website: http://www.sciencedirect.com/

[30] FERGUS, Jeffrey W. Materials Science and Engineering: A: *Review of the effect of alloy composition on the growth rates of scales formed during oxidation of gamma titanium aluminide alloys*. December 2002, [cit. 2014-02-25] Pages 108–125. Available on the website: www.sciencedirect.com

[31] GORAL, M., G. MOSKAL, L. SWADZBA. Intermetallics: *Gas phase aluminizing of TiAl intermetallics*. August 2009, [cit. 2014-05-02] Pages 669–671. Available on the website: www.sciencedirect.com

[32] Richter Precision Inc.:*PVD Coatings - Physical Vapor Deposition* [online] [cit. 2014-05-02]. Available on the website: http://www.richterprecision.com

[33] WIKIPEDIA*: Chemical Vapor Deposition*. [online]. [cit. 2014-05-02] Available on the website: http://en.wikipedia.org/wiki/Chemical_vapor_deposition

[34] NA, J., YANG, Y., LUO, X., XIA, Z. Progress in Materials Science: *Development of CVD Ti-containing films*. October 2013, 1490–1533. [cit. 2014-05-02] Available on the website: www.sciencedirect.com

8 PICTURES